Journal of Materials Chemistry B

# A Library of Aminoglycoside-derived Lipopolymer Nanoparticles for Delivery of Small Molecules and Nucleic Acids



| | |
|---|---|
| Journal: | *Journal of Materials Chemistry B* |
| Manuscript ID | TB-ART-04-2020-000924.R2 |
| Article Type: | Paper |
| Date Submitted by the Author: | 11-Aug-2020 |
| Complete List of Authors: | Godeshala, Sudhakar; Arizona State University, Chemical Engineering<br>Miryala, Bhavani; Arizona State University, Chemical Engineering<br>Dutta, Subhadeep; Arizona State University, School of Molecular Sciences<br>Christensen, Matthew; Arizona State University, Chemical Engineering<br>Nandi, Purbasha; Arizona State University, School of Molecular Sciences<br>Chiu, Po-Lin; Arizona State University, School of Molecular Sciences<br>Rege, Kaushal; Arizona State University, Chemical Engineering |
| | |

# A Library of Aminoglycoside-derived Lipopolymer Nanoparticles for Delivery of Small Molecules and Nucleic Acids

Sudhakar Godeshala[(1) (#)], Bhavani Miryala[(1) (#)], Subhadeep Dutta[(2) (#)], Matthew D. Christensen[(1)], Purbasha Nandi[(2)], Po-Lin Chiu[(2)], and Kaushal Rege[(1) (*)]

[(1)]Chemical Engineering, Arizona State University, Tempe, AZ 85287-6106 USA.
[(2)]School of Molecular Sciences, Arizona State University, Tempe, AZ 85287-6106 USA.

[(#)] Equal Contributions

[(*)]To whom all correspondence is to be addressed
Kaushal Rege
Chemical Engineering
501 E. Tyler Mall, ECG 303
Arizona State University
Tempe, AZ 85287-6106
Email: rege@asu.edu
Phone: 480-727-8616
Fax: 480-727-9321

**Keywords**: Gene delivery, neomycin, paromomycin, drug delivery, co-delivery, doxorubicin.

**ABSTRACT**

Simultaneous delivery of small molecules and nucleic acids using a single vehicle can lead to novel combination treatments and multifunctional carriers for a variety of diseases. In this study, we report a novel library of aminoglycoside-derived lipopolymers nanoparticles (LPNs) for the simultaneous delivery of different molecular cargoes including nucleic acids and small-molecules. The LPN library was screened for transgene expression efficacy following delivery of plasmid DNA, and lead LPNs that showed high transgene expression efficacies were characterized using hydrodynamic size, zeta potential, $^{1}$H NMR and FT-IR spectroscopy, and transmission electron microscopy. LPNs demonstrated significantly higher efficacies for transgene expression than 25kDa polyethyleneamine (PEI) and lipofectamine, including in presence of serum. Self-assembly of these cationic lipopolymers into nanoparticles also facilitated the delivery of small molecule drugs (e.g. doxorubicin) to cancer cells. LPNs were also employed for the simultaneous delivery of the small-molecule histone deacetylase (HDAC) inhibitor AR-42 together with plasmid DNA to cancer cells as a combination treatment approach for enhancing transgene expression. Taken together, our results indicate that aminoglycoside-derived LPNs are attractive vehicles for simultaneous delivery of imaging agents or chemotherapeutic drugs together with nucleic acids for different applications in medicine and biotechnology.

## INTRODUCTION

Multifunctional vehicles that can simultaneously deliver either multiple therapeutics or a drug along with an imaging agent can have a transformative impact in medicine [1-6]. In addition to small-molecule drugs, nucleic acids including plasmid DNA, antisense oligonucleotides, small interfering RNA (siRNA), small hairpin RNA (shRNA) and microRNA (miRNA) have emerged as promising therapeutic agents [7-11]. Non-viral vehicles typically do not approach the efficacies usually seen with viruses for efficacious nucleic acid transfer but can be engineered to possess multifunctional capabilities. In particular, delivery of nucleic acids together with small molecules either for therapeutic activity or imaging has attracted significant attention [12-14].

Polymeric nanocapsules, liposomes, dendrimers, and micelles are among the most widely investigated vehicles for delivering chemotherapeutics and biotherapeutics [15-19]. Polymeric micelles are composed of amphiphilic materials that self-assemble to form a structure which possesses a hydrophobic core and a hydrophilic corona. Hydrophobically modified water-soluble polymers [20, 21], including natural polysaccharides [22-24], are among the widely investigated drug nanocarriers [25, 26]. These carriers are typically less than 100 nm in diameter, which makes them attractive in several drug delivery applications. Polymeric micelles, in which the corona (shell) is cationic and the core is hydrophobic, are attractive for co-delivering anionic cargo (e.g. plasmid DNA) bound to the shell and small hydrophobic molecules encapsulated in the shell. Most investigations into such amphiphilic molecules [14, 27, 28] have employed existing macromolecules or their derivatives.

Aminoglycosides are a class of naturally occurring antibiotics which typically contain three to five amino substituted sugars in a single molecule and are clinically used for treating bacterial infections [29, 30]. The antibacterial activity of these molecules is derived from their ability to selectively bind bacterial ribosomal RNA [31]. Aminoglycosides are also able to bind eukaryotic RNA [32, 33] and plasmid DNA [34, 35] because of their cationic nature. We have employed aminoglycosides and their derivatives as ligands for facilitating biomolecular separations [34, 35] and DNA binding [34, 35], vehicles for DNA delivery, which results in transgene expression [36-40], drug delivery [16], and as scaffolds for cell culture [41, 42]. Quantitative Structure-Activity Relationship (QSAR) models of our first-generation aminoglycoside-derived polymer library [38] indicated that presence of moderate amounts of hydrophobicity could enhance the transgene expression efficacies of these polymers. We therefore subsequently generated lipopolymers in which, aminoglycosides were first polymerized with diglycidyl ether-based crosslinkers, and the resulting polymers were then derivatized with lipids [38]. Several among these lipopolymer candidates demonstrated transgene expression efficacies that were higher than the corresponding parental polymers.

Tumor Necrosis Factor-alpha Related Apoptosis-Inducing Ligand (TRAIL) is a protein that can induce programmed cell death in cancer cells by activating cellular apoptosis pathways upon binding cell-surface death receptors DR4 and DR5; the protein is thought to exert minimal toxicity in normal cells [43, 44]. Delivering plasmids that express the TRAIL protein is an attractive strategy for inducing death in cancer cells[45] including in human tumors grown as xenografts in mice[46]. Histone deacetylase inhibitors (HDACi) are a promising class of antitumor agents that can induce growth arrest, differentiation, and apoptosis of cancer cells through the accumulation of acetylated

histones leading to chromatin remodeling and restored transcription of genes regulating proliferation, cell-cycle progression, and cell survival [43, 47, 48]. Our previous studies showed that HDAC inhibitors were capable of increasing the transgene expression efficacy using different polymers [48, 49].

Building on these previous findings, we employed a parallel synthesis approach in order to develop a small library of aminoglycoside-derived lipopolymers that could self-assemble into nanoparticles [36, 38]. In order to accomplish this, aminoglycosides were first polymerized using a hydrophobic resorcinol-based crosslinker and the resulting polymers were derivatized with alkanoyl (acetyl, butyryl, hexanoyl, myristoyl, or stearoyl chlorides) to facilitate the formation of amphiphilic compounds. Self-assembly of these molecules in aqueous media resulted in the formation of 39 cationic lipopolymer nanoparticles (LPNs), many among which were less than 50 nm in hydrodynamic diameter. LPNs were complexed with plasmid DNA and screened for transgene expression efficacy in cancer cells. The ability of LPNs to encapsulate and deliver small molecule drugs, and facilitate the co-delivery of small-molecule drugs or dyes simultaneously with plasmid DNA was investigated using cancer cells. Taken together, our studies indicate that the library approach leads to the rapid identification of new nanoparticles for co-delivery of small-molecules and nucleic acids for different applications in biotechnology and medicine.

## EXPERIMENTAL

*Materials*

Neomycin, paromomycin, and 3.5 kDa molecular weight cutoff (MWCO)dialysis membranes were purchased from Fisher Scientific. Apramycin, resorcinol diglycidyl ether (RDE), acetyl, butyryl, hexanoyl, myristoyl, or stearoyl chlorides, triethyl amine, lipofectamine, branched poly(ethylene imine) or PEI ($M_w$ = 25 kDa and $M_n$ = 10 kDa) were purchased from Sigma-Aldrich. The HDAC inhibitor AR-42 was purchased from Selleck chemicals. Doxorubicin (free base; DOX, 99%) was purchased from Ontario Chemicals (Guelph, Ontario, Canada). All other chemicals were purchased from Sigma-Aldrich and used without further purification. The pGL4.5 control vector (plasmid DNA or pDNA), which encodes for the modified firefly luciferase protein under the control of an SV40 promoter, and the Bright-Glo$^{TM}$ luciferase assay system were purchased from Promega Corporation. The BCA protein assay kit was purchased from Thermo Scientific Inc. Full-length human TRAIL gene was first PCR-amplified from the pEGFP-TRAIL plasmid, kindly provided by Prof. Christina Voelkel-Johnson, Medical University of South Carolina, resulting in generation of the pEF-TRAIL plasmid as described in our previous studies[40]. The pEF-GFP expression vector, which expresses enhanced green fluorescent protein (EGFP) was used as a control because EGFP expression is not expected to induce death in cancer cells. Safety information for commercially available chemicals is available in MSDS sheets from the respective vendors.

*Parental Polymer and Lipopolymer Syntheses*

*Synthesis of Aminoglycoside-derived Parental Polymers.* Aminoglycoside-derived parental polymers, neomycin-RDE, paromomycin-RDE and apramycin-RDE, were synthesized and

characterized using methods described previously [36]. Briefly, the chloride forms of aminoglycosides were first treated with resorcinol diglycidyl ether (RDE) in 1:1, 1:2 and 1:2.2 molar ratios in a mixture of water and N,N-dimethylformamide (DMF) (1.5:1) and stirred for 5 hours at 60ºC. The reaction mixture was then precipitated using acetone and the semi-solid product was subsequently dialyzed using a 3.5 kDa molecular weight cutoff (MWCO) membrane in order to remove unreacted aminoglycosides and RDE. The retentate in the dialysis membrane was then lyophilized in order to obtain the final polymer product. Henceforth, the parental polymers neomycin-RDE, paromomycin-RDE, and apramycin-RDE polymers are referred to as NR, PR, and AR, respectively.

*Synthesis of Aminoglycoside-derived Lipopolymeric Nanoparticles (LPNs).* A library of 39 LPNs were synthesized using strategies shown in **Figure 1A**. The three aminoglycoside-derived polymers NR, PR, and AR were derivatized with five different alkanoyl chlorides - acetyl ($C_2$) chloride, butyryl ($C_4$) chloride, hexanoyl ($C_6$) chloride, myristoyl ($C_{14}$) chloride and stearoyl ($C_{18}$) chloride). Three different molar ratios, 1:2, 1:5, and 1:10 of the polymer:alkanoyl chloride were employed for the syntheses of 39 different LPNs (only the 1:2 and 1:5 molar ratios were used to generate acetyl chloride and butyryl chloride derived lipopolymers).

LPN syntheses were carried out following methods reported previously [36]. Briefly, 0.01 mmol of the polymer (NR, PR, or AR) were added to a small round-bottomed flask and 2 ml of DMSO were added next followed by stirring for 30 min at room temperature. To this reaction mixture, triethyl amine (0.1 mmol) was added and stirred for another 30 min. The mixture was cooled to 4ºC and different molar equivalents of alkanoyl chlorides were added drop-wise and stirred at

room temperature for 12 h resulting in the formation of 1:2, 1:5, or 1:10 lipid-conjugated polymers. The reaction mixture was then precipitated out using cold diethyl ether. The product obtained was further purified by dialysis against Milli-Q water for 48 hours using a 3.5 kDa molecular weight cutoff (MWCO) membrane. The final product was obtained after freeze drying the dialyzed material. Abbrevations and nomenclature used for all 39 lipopolymers are provided in **Table S1** (Supporting Information section).

*Characterization of Aminoglycoside-derived Lipopolymer Nanoparticles (LPNs)*

*Nucelar Magnetic Resonance (NMR) and Fourier Transform Infrared (FT-IR) Spectroscopy.* $^{1}$H NMR spectra were recorded for all parental polymers and lipopolymers, at a concentration of 10 mg/ml in DMSO-$D_6$ solvent, on a Varian 400 MHz spectrometer. All $^{1}$H NMR results were reported in δ or parts per million (ppm) units and chemical shifts were measured relative to the DMSO $^{1}$H-signal (2.50 ppm). Infrared (IR) spectra of lipopolymers (in the form of lyophilized solid powder) were measured within the range of 500-4000 $cm^{-1}$ (wave number) using FT-IR spectroscopy with a Nicolet 6700 FTIR instrument, in order to further characterize the LPNs.

*Elemental (CHN) Analyses*. Elemental analysis of selected LPNs were performed using PerkinElmer 2400 Series-II CHN analyzer system. K-factor (C: 17.5±0.15%; H: 50±3.75%; N: 6.2±0.16%) was determined as internal standard for the instrument and KASSX (C: 71±0.4%; H: 6.7±0.4%; N: 10.36±0.4%) was used for calibration. Solid (lyophilized) LPN samples (~ 4-6mg) were used for the analysis and results were reported as % weight of the C, H, and N present in the LPN samples.

*Determination of Molecular Weights (MWs)*. Lipopolymer molecular weights were determined using gel permeation chromatography (GPC) with a Waters 1515 GPC system. An aqueous solvent containing 0.1% trifluoroacetic acid (TFA) and 40% acetonitrile was used as the mobile phase with a flow rate of 0.5 ml/min. Poly(2-vinylpyridine) standards of molecular weights (MWs) 3,300, 7,600, 12,800, 35,000, and 70,000 Da (American Polymer Standards Corporation, OH) were used for calibration.

*MALDI Analyses*. Lead lipopolymers (dissolved in Milli-Q water) were analyzed using MALDI-TOF mass spectrometry (Bruker Microflex LRF MALDI-TOF instrument) before and after dialysis from a 3.5 kDa molecular weight cutoff (MWCO) tubing in order to obtain insights into composition. Briefly, 5 µl aliquots of lipopolymer samples were mixed with 5 µl matrix solution (10 mg/ml solution of α-cyano-4-hydroxy cinnamic acid (CHCA) in 50% acetonitrile with 0.1% trifluoroacetic acid (TFA)) in a microcentrifuge tube. The resultant mixture (2 µl) was applied to the MALDI sample plate and dried in vacuum before collecting the mass spectrometry data.

*Critical Micelle Concentration (CMC) analysis*. The CMC of the PR-C14 (1:2) lipopolymer in Milli-Q water was determined using a fluorescence probe technique with pyrene as a reference hydrophobic fluorescent probe [25]. Solutions of pyrene in acetone ($1.8 \times 10^{-4}$ M) were added to 20 ml vials and the acetone was removed by evaporation. Lipopolymer amounts leading to concentrations of $1.0 \times 10^{-5}$ to 1.0 mg/ml were added to the vials containing pyrene. The final concentration of pyrene in the block copolymer solutions was set at $6.0 \times 10^{-7}$ M. The solutions were stirred at room temperature for 24 h before the measurements. Excitation spectra of pyrene-

loaded nanoparticles were recorded at 390 nm using a fluorescence spectrometer at room temperature. The intensity ratio of $I_{337}$ (intensity at 337 nm wavelength) to $I_{334}$ (intensity at 334 nm wavelength) was analyzed as a function of polymer concentration in order to determine the CMC value.

*Hydrodynamic diameter, Zeta potential, and Stability of LPNs.*

Hydrodynamic diameters and zeta potential values of all 39 lipopolymers, parental polymers (NR, PR, and AR to RDE mole ratios of 1:1, 1:2 and 1:2.2) and their lipopolyplexes (1 mg/ml) in HEPES buffer (20 mM, pH 7.4) were determined using a Zetasizer Nano-ZS instrument (Malvern Instruments, Mission Viejo, CA). All nanoparticles were examined for their stability over a period of six months by determining their hydrodynamic diameters over this period.

*Lipopolyplex Visualization using Transmission Electron Microscopy (TEM).* PR-C6 (1:5) and NR-C6 (1:2) lipopolymers were incubated with the pGL4.5 plasmid for 20 min and the resulting complexes were placed onto TEM grids. Lipopolyplexes were formed using the optimal LPN:pDNA weight ratios (5:1 and 25:1) that were used in transgene expression studies (described subsequently). The samples were negatively stained with uranyl formate, and the images were acquired with a Philips CM12 transmission electron microscope (TEM), equipped with a Gatan model-791 CCD camera. Uncomplexed lipopolymers (without pGL4.5 plasmid) were also visualized.

*Transgene Expression and Cell Viability*

*Cell Culture.* Murine bladder cancer cells (MB49) were cultured in DMEM media and human prostate cancer cells (PC3, PC3-PSMA, and 22Rv1) were cultured in RPMI-1640 media, which were supplemented with 10% FBS and 1% penicillin/streptomycin solution in an incubator containing 5% $CO_2$ at 37ºC. Cells were washed with 1X PBS, trypsinized using 0.25% trypsin, seeded at a density of 9,000 cells/well in 96-well plates (Corning, Corning, NY, USA) and were allowed to attach overnight.

*Transgene expression following LPN-mediated plasmid DNA (pDNA) delivery*. All LPNs were screened in parallel for transgene expression efficacy by delivering the pGL4.5 control vector, which encodes for the modified firefly luciferase protein. The pGL4.5 plasmid DNA (pDNA) and pEF-TRAIL plasmid, which encodes for the TRAIL protein, were prepared as described previously [40]. Parent polymer nanoparticles, NR (1:1, 1:2) and PR (1:1, 1:2), were also screened separately for transgene expression efficacy by delivering the pGL4.5 control vector and by delivering pEF-TRAIL in PC3 and PC3-PSMA cancer cells. Plasmid DNA concentration and purity were obtained from a NanoDrop Spectrophotometer (ND-1000; NanoDrop Technologies) by measuring the absorbance at 260 and 280 nm wavelengths.

Luciferase (transgene) expression was determined in PC3, PC3-PSMA, 22Rv1 and MB49 murine bladder cancer cells. Initial screening of all parent polymers (NR, PR, and AR with RDE mole ratio 1:2.2) and 27 LPNs were carried out in PC3 cells; the remaining 12 LPNs were found to demonstrate larger particle sizes. Leads selected from this screen were further evaluated for their transgene expression efficacies in PC3-PSMA, 22Rv1 and MB49 cells. Lipopolyplexes (i.e.

LPN:pDNA complexes) were prepared by complexing plasmid DNA (pDNA) (75 ng) with varying amounts of LPNs in 1X PBS buffer (150 mM salt concentration, pH = 7.4) for 20 minutes. We used different LPN:pDNA weight ratios (w/w) - from 1:1 to 100:1 - for the initial screen in PC3 cells, and from 5:1 to 50:1 for evaluating lead LPNs in PC3-PSMA, 22RV1, and MB49 cells.

Cells at a density of 9,000 per well were seeded in a 96-well plate overnight, and incubated with LPN:pDNA complexes for 6 h in serum-free media after which, the media was replaced with fresh 150 µl serum-containing media. Luciferase protein expression was determined as relative luminescence units (RLU) with the Bright GloTM Luciferase assay kit (by Promega) using a plate reader (Bio-Tek Synergy 2) after 48h. Total protein content for all cell lysates was determined using the BCA Protein Assay kit (Pierce, Rockford, IL, USA). 'RLU/mg protein' luciferase expression value was calculated using normalized RLU values by the protein content in each lysate, which were employed for comparing different LPNs. Untransfected cells and cells transfected with uncomplexed ('free') pDNA were used as controls. Luciferase expression efficacies of LPNs were compared with 25 kDa branched PEI; a commonly used transfection agent with an optimized weight ratio of 1:1 in all cases [36].

*LPN-mediated Transgene Expression in Presence of Serum.* Experiments in serum-free media indicated that a 10:1 LPN:pDNA weight ratio resulted in highest efficacies of transgene expression. Consequently, this weight ratio was employed to investigate if presence of serum greatly affected transgene expression efficacy of lipopolymers. We used branched PEI as a standard for this study. All other experimental conditions were kept similar to that described in the previous section, except that serum-containing media was used instead of serum-free media.

*Evaluation of Cytotoxicity of LPNs and their Lipopolyplexes.* The cell viability of PC3 cells was determined using MTT assay following treatment with LPNs alone and also with their respective lipopolyplexes at optimal LPN: pDNA weight ratios of 5:1 to 50:1 (for all LPNs including parental polymers). Here, polymer doses of 2.5, 5, 12.5 and 25 μg/ml are equivalent to polymer:pDNA weight ratios of 5:1, 10:1, 25:1, and 50:1, respectively. The optimal LPN:pDNA weight ratio was determined from luciferase transgene expression studies. Cell seeding and lipopolyplex formation procedures were similar to those described in previous sections. Untreated cells, i.e. those only with media but no LPN or its lipopolyplex treatment, were used as controls. After 48 h of treatment, cell viability was determined as follows: the MTT (3-(4,5-dimethylthiazol-2-yl)-2,5-diphenyltetrazolium bromide) reagent (10 μl of 5 mg/ml stock) was added to all wells except for the blank wells and incubated for 3 h at 37ºC in an incubator. Next, 50 μl detergent reagent (MTT assay kit from ATCC) was added and incubated at room temperature for 5 h. After incubation, the plates were placed on a shaker in order to thoroughly mix the contents and the absorbance was determined at 570 nm using a plate reader (Bio-Tek Synergy 2). The relative cell viability (%) was calculated from $[ab]_{sample}/[ab]_{control}$ x 100%, where $[ab]_{sample}$ and $[ab]_{control}$ are the absorbance values of the wells (with LPNs or lipopolyplexes) and control wells (without LPNs or lipopolyplexes), respectively. For each sample, the cell viability was reported as the average of values measured from three wells in parallel.

*Physicochemical Characterization of LPN:Plasmid DNA Binding.*

Six LPN leads, NR-C6 (1:2), NR-C6 (1:5), PR-C6 (1:2), PR-C6 (1:5), AR-C6 (1:2), and AR-C6 (1:5) that showed high luciferase expression values and low cytotoxicity in PC3 cells were further

screened for their pDNA binding efficacies using the ethidium bromide displacement assay [35, 50]. Briefly, 1 µg of pGL4.5 and 4 µg EtBr were added to 100 µl 1X PBS (phosphate-buffered saline) buffer (pH 7.4), resulting in the formation of plasmid DNA (pDNA):EtBr complex. The fluorescence intensity value was measured using a microplate reader (FLX 800, Bio-Tek Instruments Inc., USA) with excitation at 360 nm and emission at 595 nm and noted as 100 percent fluorescence. Varying amounts of lead LPNs, corresponding to equivalents of LPN:pDNA weight ratios from 5:1 to 50:1, were added to the above pDNA:EtBr complex and equilibrated for 20 min. Fluorescence intensity was measured using 150 µl of the resulting solution in a 96-well plate. The 'percent fluorescence decreased' value was calculated for each lipopolymer by considering the fluorescence value in the absence of polymer as 100% and was used as an indicator of pDNA binding efficacy of LPNs.

*Drug Loading, Release and Cellular Uptake of LPNs*

*Preparation of Doxorubicin (DOX), HDAC inhibitor (AR-42)-loaded LPNs.* Parental polymers NR and PR with RDE mole ratios (1:1) and (1:2) were capable of forming nanoparticles by themselves. We used these polymers further for encapsulating different drugs. The free amine form of doxorubicin (DOX) (5 mg/ml) and the HDAC inhibitor (HDACi) AR-42 (5 mg/ml) were prepared in DMSO. NR, PR or PR-C14 (1:2) (5 mg) were dissolved in 0.5 ml of DMSO. To this, DOX or AR-42 dissolved in DMSO (20% by weight of the polymer), was added and the mixture was stirred at room temperature for 1 hour before being added to 3 ml Milli-Q (de-ionized) water under vigorous stirring in order to allow for encapsulation of the drugs within the nanoparticles. The dispersion was transferred to a 2 kDa molecular weight cutoff (MWCO) dialysis tubing and dialyzed against Milli-Q water at 4$^{o}$C for 24 hours; the water was changed every 3 hours and

typically, four rounds of dialysis were carried out. The solution in the tubing was lyophilized after centrifugation (4,000 rpm, for 15 min) in order to obtain drug-loaded nanoparticles. The amount of DOX encapsulated was determined by UV absorbance at 485 nm (Bio-Tek Synergy 2). The drug loading content (DLC) and encapsulation efficiency (EE) were calculated from the absorption spectra using the following equations.

DLC% = 100 * (amount of DOX within micelles / amount of DOX-loaded micelles).

EE% = 100 * (amount of DOX within micelles / amount of initial DOX used).

The amount of HDACi (i.e. AR-42) encapsulated was determined by HPLC using absorbance at 260 nm. The drug loading was calculated from the peak area of absorption spectra from HPLC.

*In vitro Doxorubicin Release*. In order to determine the release profile of doxorubicin from the lipopolymer nanoparticles, 1 ml of DOX-loaded NR (1:2), PR-C14 (1:2) nanoparticles were added into the 8-10 kDa molecular weight cutoff Float-A-Lyzer dialysis tubing (Spectrum Labs, Rancho Dominguez, CA) at 37$^{o}$C and dialyzed against 150 ml, 10 mM HEPES buffer at pH 7.4. The concentration of doxorubicin was measured at regular intervals for a period of 48 hours by carefully removing a 100 µl sample from the dialysis tubing and determining the sample absorbance. The absorbance immediately upon set up (t=0 min) was denoted as 100% doxorubicin and subsequent absorbance readings were calculated with respect to this value. Drug release was followed for up to 48 hours. Release characteristics of the free doxorubicin drug in 10 mM pH 7.4 HEPES buffer from the dialysis tubing was also determined and used for comparison with that observed with the nanoparticles.

*Cell Viability following treatment with DOX- or AR-42-loaded LPNs.* PC3 and PC3-PSMA cells were seeded at a density of 10,000 cells per well in a 96 well plate in presence of 150 µL growth

medium (RPMI / DMEM) with 10% FBS and 1% penicillin and streptomycin antibiotics. Cells were treated with various concentrations of empty (drug-free) nanoparticles, DOX or AR-42 loaded nanoparticles and incubated for 48 h or 72 h. The MTT (10 µl) reagent was added after 48 h or 72 h and incubated for 3 h at 37ºC following which, detergent reagent (50 µl) was added and incubated at room temperature for 5 h. The MTT assay data were analyzed as described previously.

*Cellular Uptake of Small Molecule-loaded LPNs.* Cellular uptake of free-base doxorubicin (DOX)-loaded LPNs was visualized by laser scanning confocal microscopy using a Leica SP5 Confocal Microscope (Leica Microsystems, Wetzlar, Germany) or a Nikon C2 laser scanning confocal system with a TE2000 inverted microscope. PC3 cells ($4 \times 10^4$) were cultured in a 24 well plate with a 1-cm diameter autoclaved coverslips for 24 hours and treated with free-base doxorubicin (DOX) in LPNs at a final DOX concentration of 13.3 µM and imaged after 24 h in order to visualize their sub-cellular localization.

Prior to imaging, cells were fixed in a 4% paraformaldehyde solution for 30 minutes followed by three washes with 1X PBS. Cells were mounted on the glass slide with glycerol-based mounting medium (90% glycerol in PBS) and imaged using Leica 40X, NA1.4 oil immersion lens or Nikon 40X, NA 1.3 oil immersion lens. Cells were excited at 480 nm (He/Ne laser) (Leica microscope) / 637 nm (Nikon microscope) and fluorescence emission was collected using a 670 nm long pass filter in order to visualize doxorubicin.

*Simultaneous Delivery of Small Molecules and Plasmid DNA using LPNs.*

We employed AR-42 loaded NR and PR nanoparticles (called as 'NR*AR*' and 'PR*AR*' to indicate loading of the *AR*-42 drug), to investigate cancer cell death following delivery of the pEF-TRAIL plasmid in PC3 and PC3-PSMA cells. Four optimal LPN:pDNA weight ratios as 10:1, 20:1, 25:1 and 50:1, were employed for these experiments. The pEF-GFP expression vector, which expresses enhanced green fluorescent protein (EGFP), was employed as a control in the study because it expresses EGFP, a protein that is not expected to induce death in cancer cells. Other experimental procedures employed in these studies were similar to those described previously in this section.

*Statistical Analyses*. All cell-based experiments were carried out at least in triplicate, and the results are expressed as mean ± one standard deviation. The Student's t-test was used to assess statistical significance of difference between group means; $p$-values $<0.05$, with respect to PEI, are considered statistically significant.

## RESULTS AND DISCUSSION

*Aminoglycoside-derived Polymers and LPNs*

Aminoglycoside-derived polymers, neomycin-RDE (NR), paromomycin-RDE (PR) and apramycin-RDE (AR) were synthesized, purified and characterized using previously described methods[36]; approximate yields for the parental polymers ranged from 40-50%. LPNs were synthesized by reacting amines of parental polymers NR, PR, and AR with different lipids including acetyl ($C_2$), butyryl ($C_4$), hexanoyl ($C_6$), myristoyl ($C_{14}$) and stearoyl ($C_{18}$) chlorides (**Figure 1**). We employed different alkanoyl groups with different chain lengths in order to systematically modulate the hydrophobicity and nanoparticle-forming propensity of the resulting

polymers. A total of 39 different LPNs were synthesized using different polymer:lipid reaction molar ratios (1:2, 1:5 and 1:10) and purified with average yields ranging from 30-55% (**Table S1**, Supporting Information section).

*Characterization of Lipopolymer Formation*

*Nucelar Magnetic Resonance (NMR) and Fourier Transform Infrared (FT-IR) Spectroscopy.* $^{1}$H NMR analysis in **Figure S1** (Supporting Information section) indicated the presence of alkanoyl protons such as $–CH_3$ (marked as 'a' at δ 0.8 ppm), γ-$CH_2$ and β-$CH_2$ (marked as 'b' at the range of δ 1.2-1.6 ppm), α-$CH_2$ (marked as 'd' at δ 2.16 ppm) in the LPNs, which in turn, are indicative of the conjugation of lipid onto the aminoglycoside-derived parental polymers. The $^{1}$H NMR spectra of the PR polymer and its derivative PR-C14 (1:2) formed by $C_{14}$ lipid-conjugation is shown in the **Figure S1** (Supporting Information section) as a representative example; the nomenclature system for LPNs is described in **Table S1** (Supporting Information section). The integrated values of the characteristic resonance shifts corresponding to lipid acid chloride (δ ~ 0.8 ppm, -C$H_3$) and aminoglycoside-derived polymer (δ ~ 7.1-7.2 ppm, -C$H_{\text{Benzene}}$) were used to obtain the extent of lipid substitution for a given lipopolymer (**Table S2**, Supporting Information section). The information in **Table S2** shows the reaction molar ratios, the ratios calculated from NMR and the degree of lipid substitution of the LPNs. As seen in the table, the number of grafted lipids generally increased with increasing reaction molar ratios. The FTIR spectra of the parental polymer PR and its corresponding lipopolymer PR-C6 (1:2) formed by $C_6$ lipid-conjugation are shown in **Figure S2** (Supporting Information section). The peaks for N-H and O-H stretching overlapped to form a broad peak at 3418 $cm^{-1}$. The % transmittance of alkyl C-H ($sp^3$) stretching at 2935 $cm^{-1}$ in LPN's FTIR spectrum was higher compared to that seen for the parental polymer,

which indicated presence of the lipid acid chlorides in the lipopolymer nanoparticles. Amide linkages between parental aminoglycoside polymers and the lipids were identified at 1668 $cm^{-1}$, which further indicated conjugation of lipids.

*Elemental Analyses.* Elemental analyses with select LPNs indicated an increase in weight percentage of carbon (C) and hydrogen (H) compared to their corresponding parental polymer samples (**Table S3**, Supporting Information section). In contrast, the weight percent of nitrogen (N) in LPNs was lower than in parental polymers. This is consistent with the conjugation of the lipids onto parental polymers which results in an increase in carbon and hydrogen but not nitrogen, thus accounting for the observations seen in the elemental analyses.

*Determination of Molecular weights (MWs)of LPNs.* Gel Permeation Chromatography (GPC) analyses indicated that the average molecular weights of polymer or lipopolymer molecular weights and polydispersities were in the range of 3.2-5.3 kDa, and 1.1-1.3, respectively (**Table S4**, Supporting Information section). Mass spectrometry using MALDI-TOF analyses with lipopolymer reaction mixture pre- and post-dialysis (retentate) indicated that the process was able to remove low molecular weight constituents like excess lipid acid chlorides (**Figure S9**, Supporting Information section). It is likely that some parental polymer is present in the retentate post-dialysis.

*Nanoparticle Formation Studies*

Parental polymers and aminoglycoside-derived lipopolymers form self-assembled nanoparticles by themselves (**Figure 2**). Parental polymers NR (1:1, 1:2) and PR (1:1, 1:2), formed nanoparticles

with hydrodynamic diameters in the range of 120-190 nm and zeta potential values in the range of 5-20 mV in Milli-Q water (with pH 8-8.5). All alkanoyl derivatives of the parental aminoglycoside-derived polymers also self-assembled into nanoparticles with hydrodynamic diameters in the range of 20-170 nm and zeta potential values in the range of 0.2-50 mV (**Figure 2**). LPNs derived from the AR polymer possessed lower hydrodynamic diameters when compared to those derived from NR and PR polymers. In general, it was found that LPNs derived using longer lipid chains and from higher reaction molar ratios (i.e. 1:10 of polymer:lipid) were larger in size when compared to those of lower reaction molar ratios (1:2 and 1:5). Zeta potential values increased with molar ratios employed in the conjugation reaction of lipids onto the parental polymer. Higher lipid:polymer molar ratios are likely to result in a reduction in the number of primary amines, which in turn can cause a reduction in the nanoparticle zeta potential values. The critical micellar concentration or CMC of PR-C14 (1:2) lipopolymer was determined using the pyrene fluorescence assay (**Figure S3**, Supporting Information section). The CMC analysis further indicates the formation of nanoparticles.

Stability of polymeric nanoparticles was determined by determining their hydrodynamic diameters over time. All LPNs were stable for at least one week whereas drug (doxorubicin or AR-42) loaded nanoparticles were stable for up to one week. The lead lipopolymer PR-C14, i.e. PR polymer conjugated with $C_{14}$ lipid, was stable for over a period of 6 months in 20 mM HEPES buffer (pH 7.4) when stored at 4$^{o}$C (**Figure S4**, Supporting Information section).

*Characterization of Lipopolyplexes*

*Hydrodynamic Diameters, Zeta Potential Values, Transmission Electron Microscopy of LPN:pDNA Lipopolyplexes*. The hydrodynamic diameters and zeta potential values of LPN:pDNA complexes were determined for LPN:pDNA weight ratios of 5:1 to 50:1, which were used for transgene expression (**Figure 4**). Hydrodynamic diameters ranging from 50 nm to 1600 nm were observed, and complexes formed at lower weight ratios of 5:1 and 10:1 were generally larger than the complexes formed at higher weight ratios of 25:1 and 50:1 (**Table 1**). This is likely because of the lower amine content at lower weight ratios, which may result in inefficient complexation. The reduction in complex size at higher weight ratios (approximately 40-60 nm) can also be attributed to the increased lipid content which facilitates stronger hydrophobic association, and therefore, compaction of the complexes [51, 52]. Zeta potential values of LPN:pDNA complexes ranged from of +0.2 to +50 mV, and typically increased with increasing amount of LPN employed in the complexes (**Table 1**). This is along expected lines, because increasing the cationic content from LPNs is required to neutralize the anionic content from DNA molecules.

Transmission electron microscopy (TEM) visualization of negatively stained uncomplexed LPNs and LPNs complexed with pGL4.5 pDNA indicated relatively uniform dimensions of the particles formed in each case (**Figure 3**); the particles appear white on black background. Particles appear well dispersed in case of uncomplexed LPN and LPN complexed with pDNA at a weight ratio of 5:1. Some clustering of particles was observed at the higher LPD:pGL4.5 weight ratio of 25:1, likely because of bridging and other artefacts during drying on the TEM grid[53].

*LPN-mediated Plasmid DNA (Gene) Delivery: Transgene Expression and Cell Viability*

*Transgene (luciferase) expression following LPN-mediated plasmid DNA (pDNA) delivery.* A library of 39 LPNs **Table S1** (Supporting Information section) was screened for luciferase transgene expression following delivery of the pGL4.5 plasmid to PC3 cells. LPN:pDNA weight ratios ranging from 1:1 to 100:1 were employed in the initial screening [**Figure 4 (A-C)**]. In addition, parental polymer nanoparticles [NR (1:1, 1:2) and PR (1:1, 1:2)][38], and lipofectamine, a commercial transfection agent (**Figure S5**), were also evaluated for transgene expression efficacy. A significant increase in luciferase protein expression was observed for several LPNs compared to 25 kDa PEI, lipofectamine or the corresponding parental aminoglycoside-derived polymers in the primary screening [**Figure 4 (A-C)**]. PR- and AR-derived LPNs showed higher levels of luciferase expression compared to those derived from NR. An increase in luciferase expression of 1.5-2 fold was observed in case of PR- and AR-derived LPNs compared to their parental polymers, but a significant increase was not seen in case of NR-derived LPNs. In general, derivatization with hexanoyl ($C_6$) moieties enhanced transgene expression, likely because of an optimized balance between the hydrophobicity of this group along with that of the cross-linker and the cationic charge on the lipopolymers. Thus, lipid-conjugation generally improves the efficacy of aminoglycoside-derived nanoparticles, which is consistent with other observations in the literature [36, 54-58].

The hydrodynamic diameter and zeta potential values of LPNs (**Table 1**) also correlate with transgene expression efficacies observed with LPNs. Weight ratios that result in complexes less than 200 nm in diameter and generally cationic zeta potential values demonstrated among the highest levels of luciferase expression in **Figure 4 (A-C)**. This is likely because optimal zeta potential and particle size values can promote effective uptake, trafficking and transgene

expression following delivery of LPN:pDNA complexes. Taken together, LPN and lipopolyplex chemistries and physicochemical properties determine effective transgene expression following complexation and delivery of plasmid DNA. However, detailed structure-property investigations are needed in order to further elucidate physicochemical and cellular factors responsible for this activity.

Screening results in **Figure 4 (A-C)** also indicate that LPN:pGL4.5 weight ratios from 5:1 to 50:1 generally resulted in the highest levels of luciferase expression. Although the optimal ratio was a function of polymer and lipid chemistry, a weight ratio of 10:1 was generally found to be most effective across different LPNs. LPNs containing $C_6$ lipids at all three molar ratios and $C_{14}$ lipids at lower molar ratios of 1:2 and 1:5 demonstrated higher levels of luciferase expression compared to those containing $C_{18}$ moieties. This is likely because the 1:2 and 1:5 polymer : lipid derivatives balance hydrophobic character of the lipids with electrostatic charge from the amines. Increasing the number of lipid molecules destroys the cationic character of the parental polymers due to increased consumption of amines in the reaction, and likely leads to lower efficacies. These results are also consistent with previous reports which indicate dependence of transgene expression efficacy on length and extent of the lipid conjugated [59, 60].

*Evaluation of Lead LPNs for Transgene Expression*. Six LPNs, NR-C6 (1:2), NR-C6 (1:5), PR-C6 (1:2), PR-C6 (1:5), AR-C6 (1:2) and AR-C6 (1:5), were selected from initial screening of luciferase expression and subjected to subsequent investigations. Lead LPNs were further evaluated for *in vitro* transgene expression efficacy in three additional cell lines including 22Rv1 (human prostate cancer), PC3-PSMA (human prostate cancer) and MB49 (murine bladder cancer)

at different weight ratios (5:1 to 50:1). NR-C6 (1:2) and NR-C6 (1:5) demonstrated higher luciferase expression in 22Rv1 cells compared to LPNs derived from PR and AR polymers PR-C6 (1:2) and AR-C6 (1:2) [**Figure 5 (A-C)**]. However, AR-derived LPNs demonstrated higher levels of luciferase expression than those derived from PR in PC3-PSMA cells [**Figure 5 (A-C)**]. It was found that in case of luciferase expression, the most effective weight ratios and the fold-enhancement of lipopolymers compared to parent polymers were dependent on the cell type, which is consistent with previous reports in literature [61]. The highest fold enhancement (1.5-fold) for NR-derived LPNs over the corresponding NR polymer was in 22Rv1 cells. In the case of PR- and AR-derived LPNs, the enhancement was 2-fold and was observed in PC3, 22Rv1, MB49 cells and PC3-PSMA cells, respectively.

*LPN-mediated transgene expression in presence of serum*. Presence of serum can strongly inhibit transgene expression following plasmid DNA delivery by non-viral vectors [62, 63]. Serum incompatibility typically arises from adsorption of negatively charged serum proteins to cationic moieties, which can destabilize polymer / lipopolymer : pDNA complexes resulting in reduced efficacies [64]. **Figure 6** shows that NR- and PR-derived LPNs demonstrated high efficacies of transgene expression even in presence of 10% serum. A decrease in luciferase expression to the extent of 50%, 30-40%, and 10-20% were observed with AR-C6 (1:2), PR-derived LPNs, and NR-derived LPNs, respectively. At serum levels of 30% and 50%, luciferase expression following pDNA delivery with NR- and PR-derived LPNs was largely invariant, whereas a significant decrease was observed with AR-derived LPNs compared to serum-free conditions. NR and PR-derived LPNs resulted in higher luciferase expression than 25 kDa PEI across all concentrations

of serum tested. The observed stability in serum and improved performance over PEI, further indicate the promise of LPNs for transgene delivery and expression.

*Cytotoxicity of LPNs and LPN:pDNA Lipopolyplexes*

LPN lipopolyplexes demonstrated minimal toxicity towards PC3 cells at weight ratios of 5:1, but significant toxicities were seen when weight ratios of 50:1 were employed (**Figure S7 A-C**; Supporting Information section). It is likely that higher concentrations of LPNs induce membrane disruption of target cells, ultimately resulting in a loss of cell viability[65]. Cytotoxicity was dependent on the type of LPN employed for weight ratios of 10:1 and 25:1. AR-derived LPN-lipopolyplexes demonstrated higher cell viabilities, but no general trend was found with respect to the chain length of the conjugated lipid employed in LPN generation. These results are also consistent with transgene expression results observed with different cells; weight ratios that resulted in significant loss of viability expectedly resulted in poorer levels of transgene expression. Free LPNs, uncomplexed with pDNA, demonstrated similar levels of toxicity towards PC3 cells as seen with LPN:pDNA lipopolyplexes [**Figure S6 (A-C)**, Supporting Information section]. As expected, higher loss in viability was seen when cells were treated with higher concentrations of LPNs (25 µg/ml LPN dose, which was equivalent to that used in LPN:pDNA weight ratios of 50:1).

*Plasmid DNA binding Efficacy of Lead LPNs.* The percentage fluorescence decrease in the ethidium bromide displacement assay is an effective indicator of the DNA binding efficacy of molecules[34, 35]. **Figure S8** (Supporting Information section) indicates that % fluorescence decrease is higher for LPNs compared to parental polymers at higher weight ratios of 50:1.

However, at lower weight ratios of 5:1 to 25:1 the percentage decrease of fluorescence intensity is comparable between LPNs and their parental polymers. The pDNA binding efficacy of polymers can be varied by varying the extent of lipid conjugation on parent polymers, which is an approach that substitutes amine moieties with lipid molecules [66]. Presence of the hydrophobic (lipid) moieties can further help displace ethidium bromide from its hydrophobic environment in the DNA leading to increase in % fluorescence decreased particularly at higher LPN amounts. Taken together, these studies verify that LPNs indeed bind pDNA and that these interactions are strong enough to displace the intercalating ethidium bromide dye from the plasmid DNA.

*Small Molecule Delivery using LPNs*

*Doxorubicin (DOX)-loaded Nanoparticles: Preparation, Drug release and Cytotoxicity.* We next investigated the ability of parental polymer [NR (1:1) and NR (1:2)] and lipopolymer nanoparticles [LPNs; PR-C14 (1:2)] for delivering small molecules (drugs) to cells as an additional application of these versatile materials. Doxorubicin (DOX) is a widely investigated hydrophobic anti-cancer therapeutic, and was therefore used as a model small molecule drug for encapsulation within parent polymeric nanoparticles and LPNs in the current studies. Furthermore, DOX possesses strong fluorescence properties which facilitates sub-cellular visualization[67]. The drug loading capacities of DOX for NR (1:1) and NR (1:2) were found to be 5.5% and 7.3% respectively, and the drug encapsulation efficacy of DOX for NR (1:1) and NR (1:2) were found to be 33.1% and 43.9% respectively, whereas drug loading capacity and encapsulation efficacy of DOX for PR-C14 (1:2) was found to be 9.5% and 57.2% respectively, indicating that the drug was encapsulated in both polymer [NR (1:1) and NR (1:2)] and lipopolymer PR-C14 (1:2). **Figure 7 (A-D)** shows that the cytotoxicity of (DOX)-loaded NR (1:2) nanoparticles was higher than that of NR (1:1)

nanoparticles and unloaded (empty) NR (1:1) and NR (1:2) nanoparticles in both PC3 and PC3-PSMA cancer cells treated for 48h and 72h.

*In vitro drug release. In vitro* drug release of DOX from NR (1:2), PR-C14 (1:2) LPNs was investigated using a dialysis membrane in 10 mM HEPES (pH 7.4) and compared with the diffusion of free DOX through the membrane. As shown in **Figure 8**, only 10-20% DOX was lost from nanoparticles over a period of 48 h, confirming the DOX encapsulated within polymeric hydrophobic micelle cores. The release of free DOX (in 10 mM HEPES buffer) was found to be 90% over a period of 48 h, which is along expected lines for unencapsulated drug molecules.

*Cellular uptake of DOX-loaded LPNs*. Cellular uptake of doxorubicin-loaded LPNs was visualized using confocal fluorescence microscopy. Following 24 h treatment, DOX-loaded NR (1:2), DOX-loaded PR-C14 (1:2) LPNs, as well as free DOX (not encapsulated within LPNs) were observed both in the cytoplasm as well as the nucleus of PC3 cells (**Figure 9**), likely due to passive diffusion of the drug [68]. These results indicate that LPNs can be used for cellular delivery of small molecule drugs, likely because positive charges on the nanoparticles aid their uptake due to electrostatic interactions with cell membranes.

*Combined Gene and Drug Delivery using LPNs*

Histone deacetylases (HDACs) are overexpressed in several cancers and the inhibition of these enzymes is an attractive approach for cancer cell ablation [47, 48]. A histone deacetylase (HDAC) inhibitor, AR-42, was loaded (20% w/w) in NR (1:2) polymer, which resulted in the formation of AR-42 loaded NR nanoparticles (NRAR). The loading of HDACi (AR-42) in LPNs, determined

using HPLC in concert with absorbance at a wavelength of 260 nm, was found to be 5.9%. NRAR nanoparticles were further investigated for simultaneous delivery of drug (AR-42) and pEF-TRAIL plasmid in PC3 and PC3-PSMA cells. The nanoparticles were complexed with plasmid DNA (pEF-TRAIL or pEF-GFP) at polymer:pDNA weight ratios of 10:1, 20:1, 25:1 or 50:1; the pEF-GFP expression vector, which expresses enhanced green fluorescent protein (EGFP), was employed as a control in the study. In particular, the NRAR:pTRAIL complex of weight ratio 50:1 was effective in ablating both PC3 and PC3-PSMA cancer, and lead to death in approximately 60-70 % cancer cells (**Figure 10**). In comparison, the NRAR+pEGFP (no TRAIL) and NR+pTRAIL (no AR-42 drug) controls were not able to induce as high a loss in cell viability (~ 28% and 32% death) as the combination NRAR:pTRAIL treatment, indicating the efficacy of the combination treatment approach.

## CONCLUSIONS

In this study, we synthesized and characterized a library of 39 lipopolymer nanoparticles (LPNs) for simultaneous nucleic acid and small-molecule delivery. LPNs possessed nanoscale hydrodynamic diameters and positive surface charges, which resulted in high efficacies for complexing and delivering plasmid DNA and concomitant high levels of luciferase expression. Complexation of LPNs with plasmid DNA resulted in nanoparticle ('lipopolyplex') formation as determined using dynamic light scattering and transmission electron microscopy studies. LPNs demonstrate high efficacies of transgene expression even in presence of high amounts of serum; this was not seen with PEI, which is a commonly used commonly used polymer for pDNA delivery. In addition, LPNs demonstrated an ability to carry and deliver small-molecule chemotherapeutic drugs, including in concert with plasmid DNA, leading to combination drug and

nucleic acid delivery systems. In summary, the current library of aminoglycoside-derived LPNs are promising nanoscale vehicles for drug, nucleic acid, or simultaneous small-molecule and nucleic acid delivery for a variety of biomedical applications.

## ACKNOWLEDGEMENTS

We are grateful to the NIH/NIGMS (Grant 1R01GM093229-01A1), Arizona Biomedical Research Commission (ABRC; ADHS14-082981), and National Science Foundation (Grant 1836525) for funding this study. We are thankful to Professor Deirdre Meldrum, Center for Biosignatures Discovery Automation (CBDA), for access to the Zetasizer Nano-ZS instrument and to Dr. Yanqing Tian, CBDA, for several helpful technical discussions. We also thank Dr. Page Baluch at the Regenerative Medicine and Bioimaging facility at Arizona State University for her invaluable help with confocal microscopy. The authors also acknowledge resources and support from the Magnetic Resonance Research Center (MRRC); Eyring Materials Center; and the Metals, Environmental and Terrestrial Analytical Laboratory; which are part of the Core Facilities at Arizona State University.

## SUPPORTING INFORMATION

Characteristic $^{1}$H-NMR spectra of polymers and their derivative LPNs, table showing the degree of substitution of lipids on polymers, and additional characterization and evaluation of LPNs are included in the Supporting Information section.

## CONFLICT OF INTEREST

Prof. Rege is affiliated with a start-up company, Synergyan, LLC

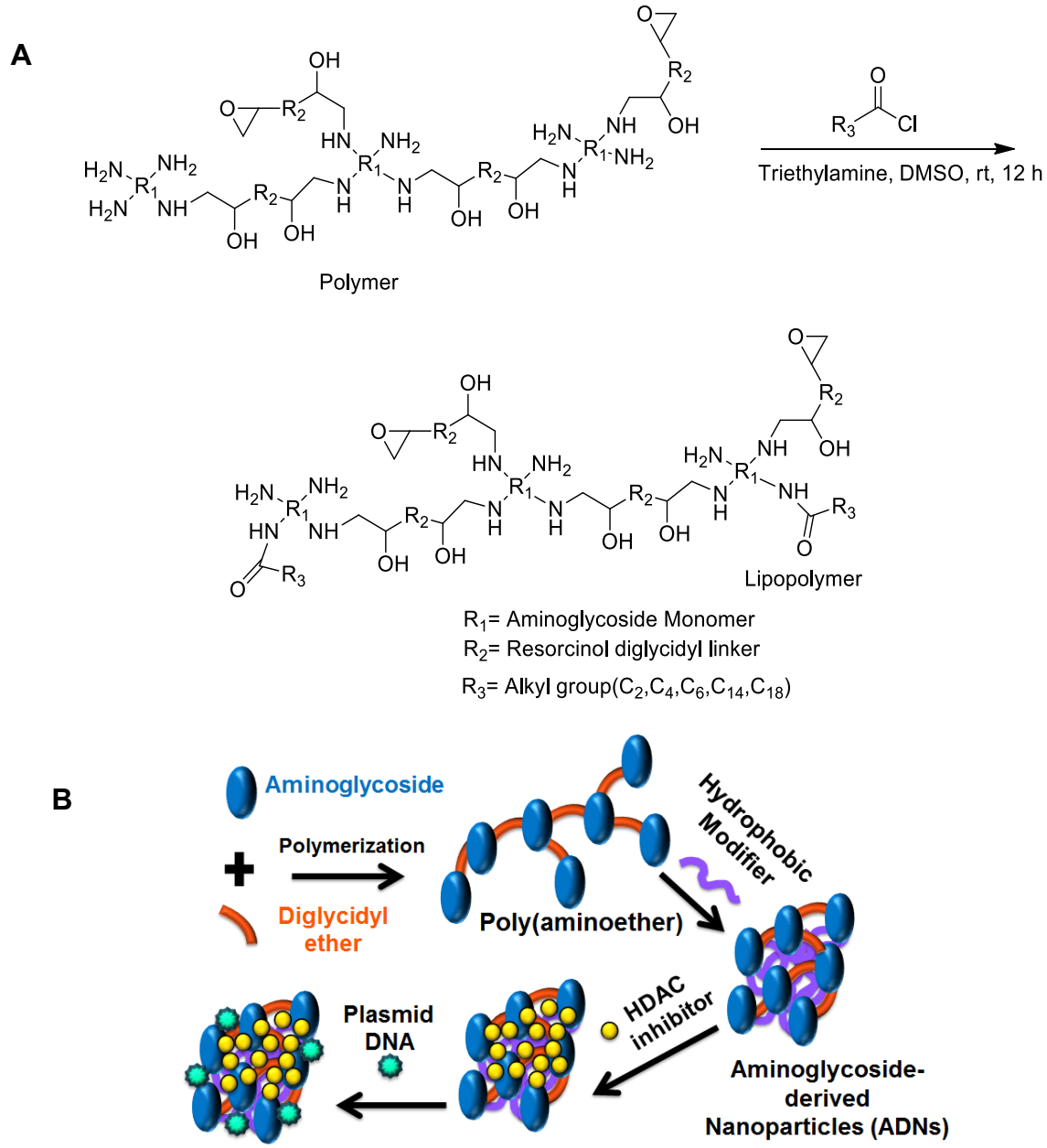


**Figure 1. (A)** Schematic illustration of lipopolymer formation by derivatizing aminoglycoside-derived NR, PR, and AR polymers with different alkanoyl ($C_2$, $C_4$, $C_6$, $C_{14}$, and $C_{18}$) chlorides. This scheme is intended to only show the general reaction and does not represent the exact mechanism by which this reaction proceeds. **(B)** Schematic illustration of self-assembled lipopolymer nanoparticles (LPNs) for simultaneous delivery of small molecules (e.g. HDAC inhibitors) and nucleic acids (e.g. plasmid DNA). Some parental polymers spontaneously form nanoparticles without the need for a hydrophobic modifier.

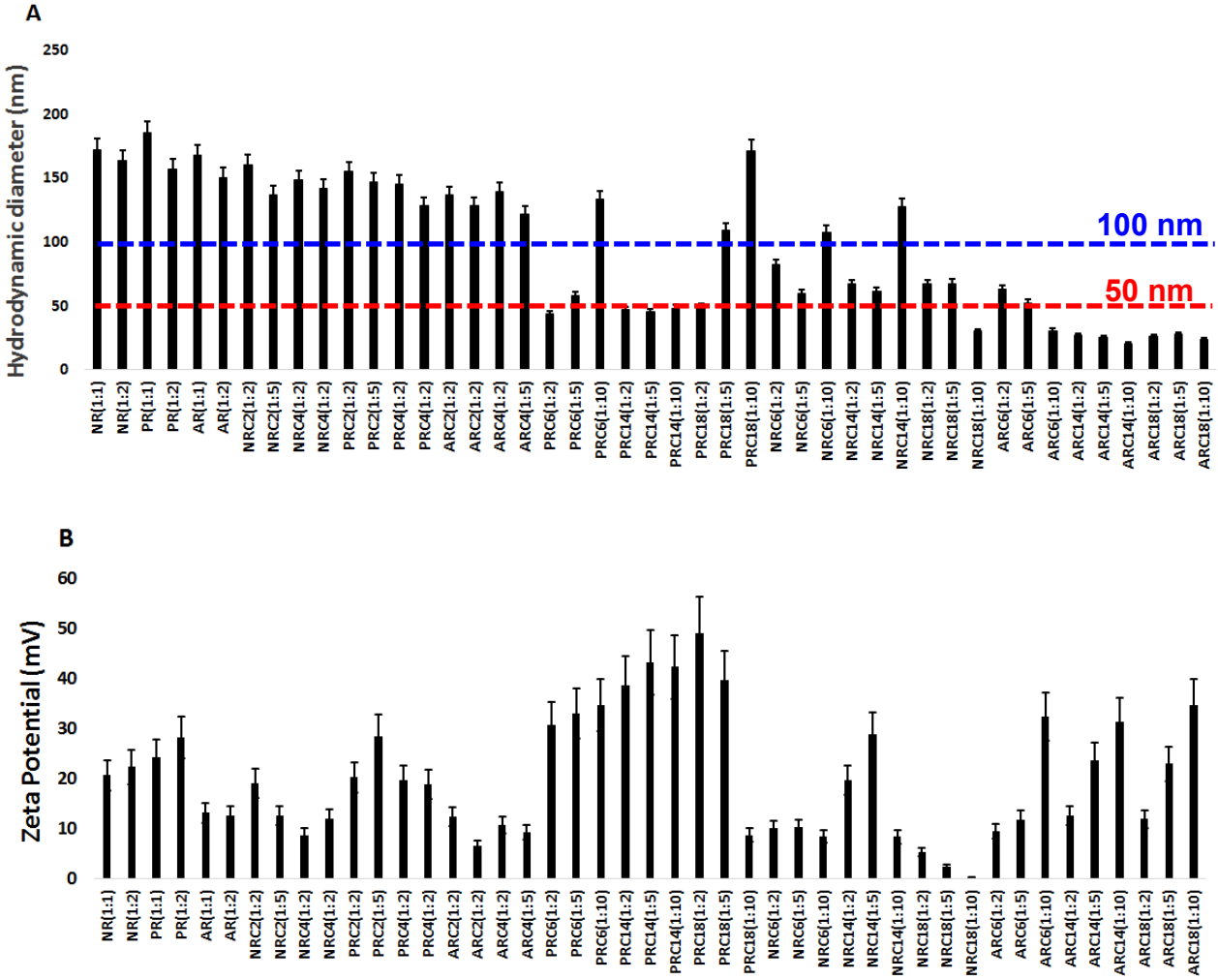


**Figure 2. (A)** Hydrodynamic diameters (nm) and **(B)** and zeta potential values (mV) of parental polymers and LPNs determined in 20 mM HEPES buffer (pH 7.4) uncomplexed with plasmid DNA. Please see the experimental section for details.

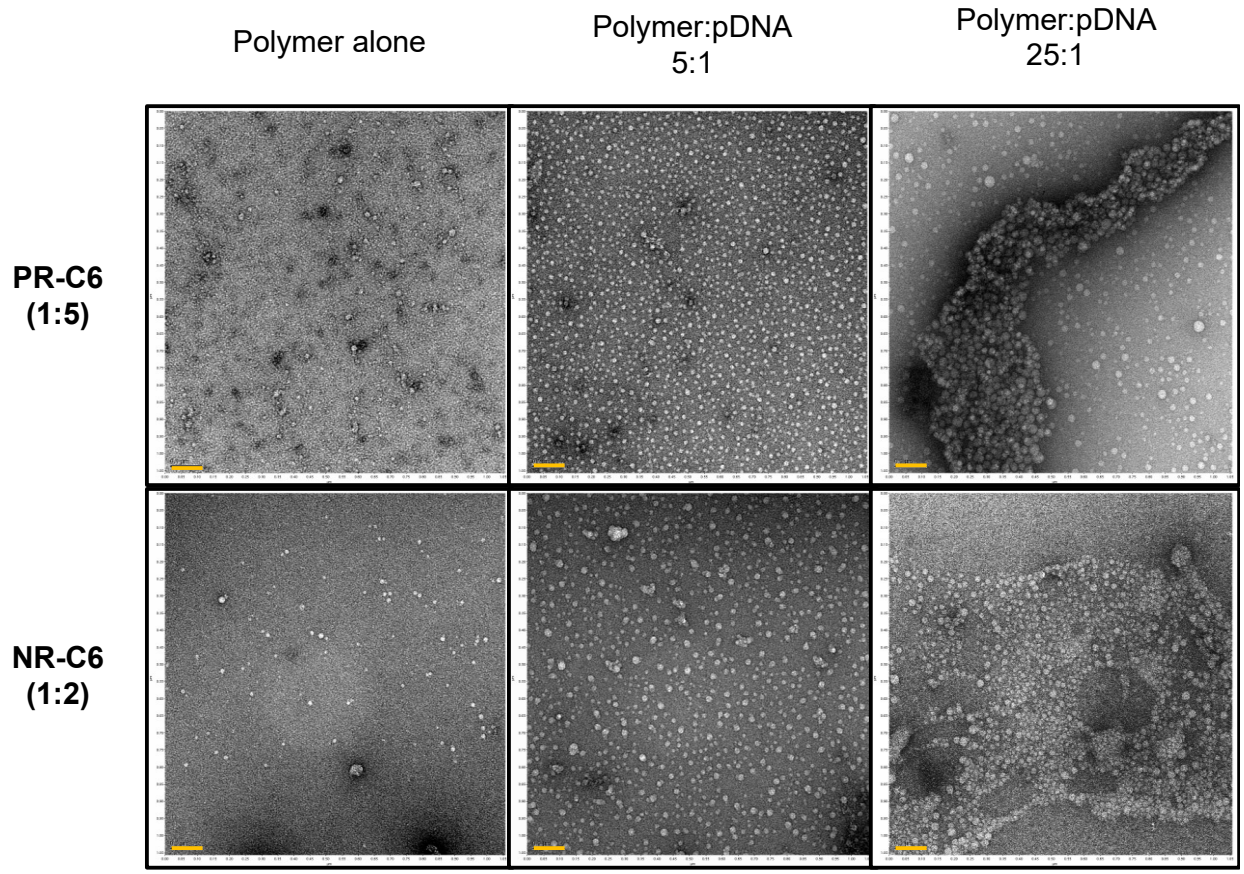


**Figure 3.** Electron micrographs of the negatively stained lead lipopolymer nanoparticles (LPNs) PR-C6 (1:5) and NR-C6 (1:2) and their respective lipopolyplexes at LPN:pDNA ratios of 5:1 and 25:1. White color indicates LPNs or LPN:pDNA complexes and black color indicates negative-stained background in the image. Scale bars in yellow indicate 100 nm in all images.

| | LPN: pDNA (weight ratio) | | | | |
|---|---|---|---|---|---|
| **LPN** | 1:0 | 5:1 | 10:1 | 25:1 | 50:1 |
| | **Hydrodynamic Diameter (nm)** | | | | |
| NR (1:1) | 369±3 | 453±3 | 429±4 | 231±5 | 193±3 |
| NR (1:2) | 344±3 | 422±4 | 322±3 | 190±4 | 185±3 |
| PR (1:1) | 445±4 | 365±4 | 334±5 | 187±6 | 194±3 |
| PR (1:2) | 433±5 | 387±6 | 318±4 | 175±2 | 174±5 |
| NR-C6 (1:2) | 41±1 | 323±1 | 405±6 | 131±5 | 97±1 |
| NR-C6 (1:5) | 40±1 | 704±32 | 205±1 | 66±1 | 49±1 |
| PR-C6 (1:2) | 14±3 | 281±28 | 1175±14 | 76±2 | 79±2 |
| PR-C6 (1:5) | 25±1. | 907±113 | 79±1 | 61±1 | 67±5 |
| AR-C6 (1:2) | 29±7 | 108±1 | 925±36 | 94±1 | 47±1 |
| AR-C6 (1:5) | 34±1 | 95±4 | 1622±83 | 85±1 | 48±1 |
| | **Zeta Potential (mV)** | | | | |
| NR (1:1) | 12±4 | 19±2 | 16±5 | 21±1 | 23±4 |
| NR (1:2) | 15±2 | 16±4 | 19±2 | 25±4 | 27±4 |
| PR (1:1) | 16±3 | 16±2 | 18±3 | 20±4 | 21±2 |
| PR (1:2) | 12±3 | 13±3 | 16±3 | 21±2 | 22±4 |
| NR-C6 (1:2) | 29±2 | 12±1 | 19±2 | 31±1 | 33±1 |
| NR-C6 (1:5) | 29±1 | 17±1 | 17±1 | 29±1 | 32±6 |
| PR-C6 (1:2) | 24±6 | 10±2 | 10±1 | 32±1 | 35±1 |
| PR-C6 (1:5) | 27±2 | 5±1 | 14±1 | 35±1 | 36±1 |
| AR-C6 (1:2) | 21±1 | 2±1 | 17±4 | 19±1 | 27±3 |
| AR-C6 (1:5) | 24±5 | 11±1 | 15±1 | 20±1 | 30±1 |

**Table 1.** Hydrodynamic diameter (nm) and zeta potential values (mV) of lead LPNs and LPN:pDNA complexes (lipopolyplexes).*

*Complexes were formed at optimal LPN:pDNA weight ratios of 5:1 to 50:1 (chosen from initial screening of lipopolymers in PC3 cells) by incubating with 100 ng of pDNA for 20 minutes before measuring lipopolyplex size and zeta potential. Measurements were carried out in 1X PBS buffer (150 mM salt concentration, pH 7.4). The first column in the table ("1:0") indicates properties of the LPNs alone, which verifies that these delivery vehicles self-assemble into nanoparticles by themselves (i.e. in absence of plasmid DNA).

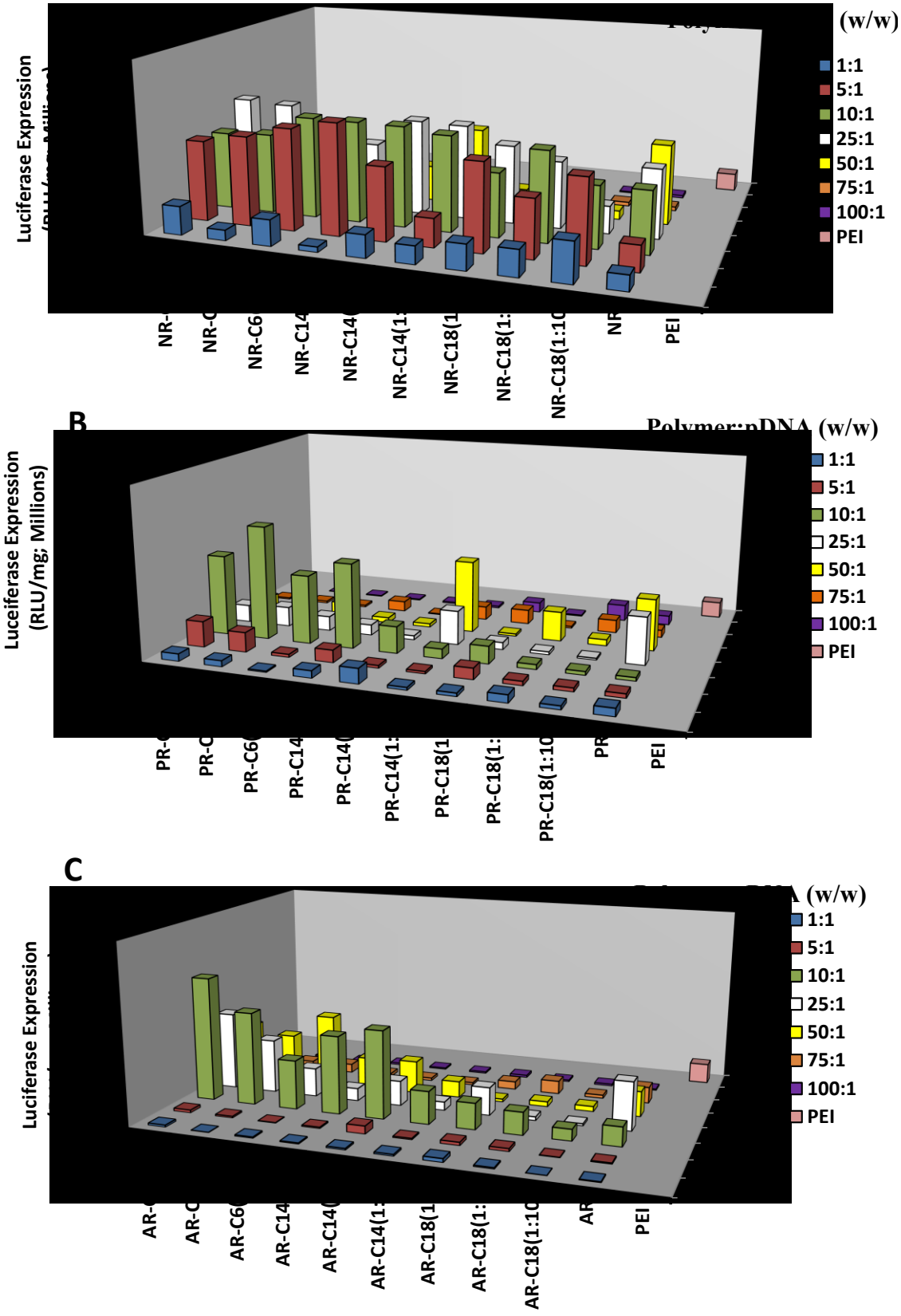
Luciferase Expression
(w/w)
1:1
5:1
10:1
25:1
50:1
75:1
100:1
PEI
NR-C18(1:10
B
Luciferase Expression
(RLU/mg; Millions)
Polymer:pDNA (w/w)
PR-C18(1:10
C
Luciferase Expression
AR-C18(1:10

**Figure 4.** Transgene (luciferase) expression following delivery of pGL4.5 plasmid DNA (pDNA) to PC3 cells using **(A)** NR polymer **(B)** PR polymer, and **(C)** AR polymer, and their respective derivatives with three different lipids ($C_6$, $C_{14}$, and $C_{18}$) each at three different molar ratios. Luciferase expression was evaluated for 1:1 to 100:1 lipopolymer:pDNA (w/w). Transgene expression efficacies of lipopolymers were quantified in terms of relative luciferase units (RLU) and normalized to total protein content (mg), resulting in RLU/mg values. Transgene expression efficacies of lipopolymers were compared with that of parental NR, PR, and AR polymers in addition to 25 kDa branched poly(ethyleneimine) (PEI). Experiments were carried out in triplicate and mean values from these are shown (n=3 independent experiments; error bars are not shown).

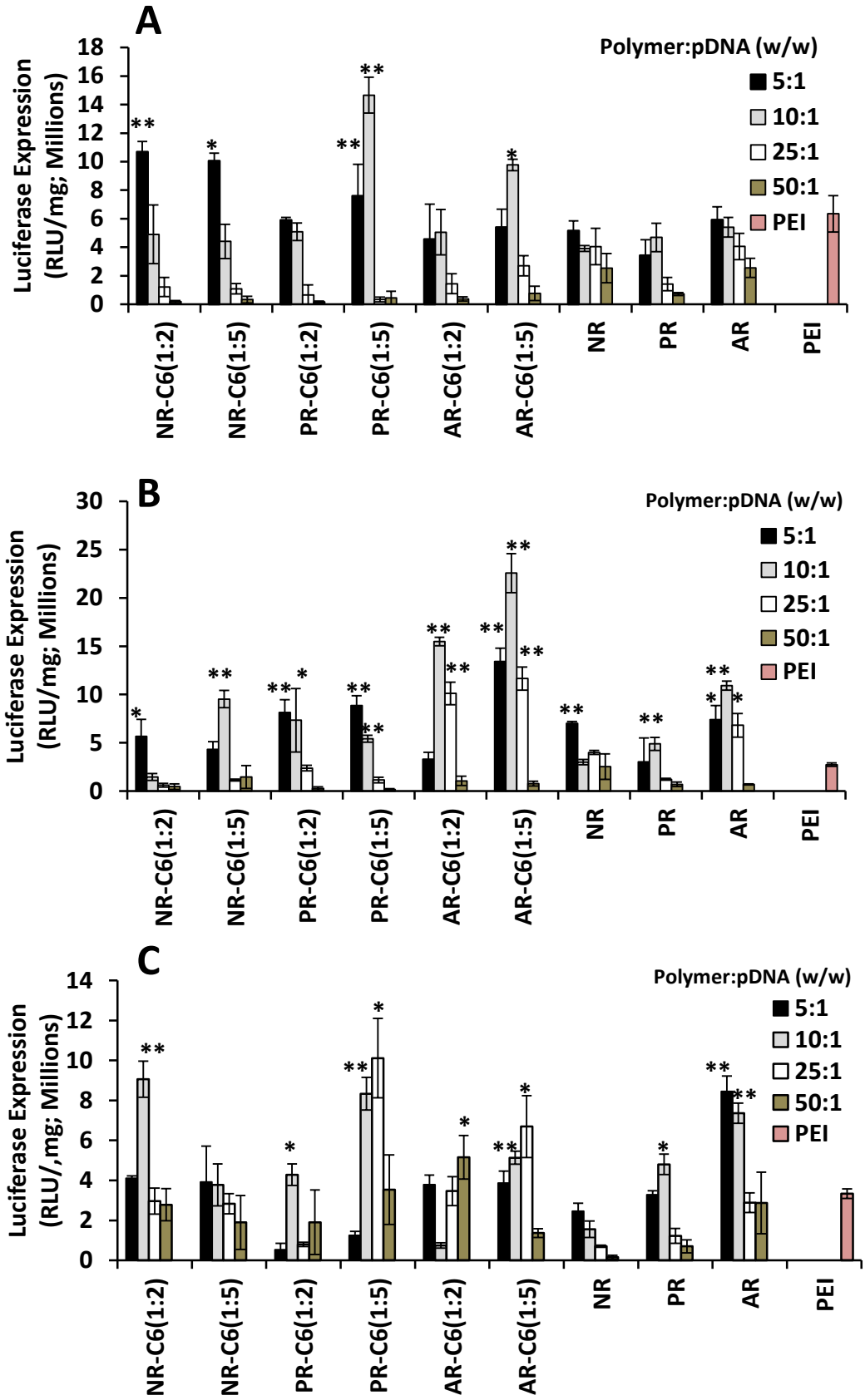
A
Luciferase Expression (RLU/mg; Millions)
Polymer:pDNA (w/w)
5:1
10:1
25:1
50:1
PEI
NR-C6(1:2)
NR-C6(1:5)
PR-C6(1:2)
PR-C6(1:5)
AR-C6(1:2)
AR-C6(1:5)
NR
PR
AR
PEI
B
Luciferase Expression (RLU/mg; Millions)
Polymer:pDNA (w/w)
5:1
10:1
25:1
50:1
PEI
NR-C6(1:2)
NR-C6(1:5)
PR-C6(1:2)
PR-C6(1:5)
AR-C6(1:2)
AR-C6(1:5)
NR
PR
AR
PEI
C
Luciferase Expression (RLU/,mg; Millions)
Polymer:pDNA (w/w)
5:1
10:1
25:1
50:1
PEI
NR-C6(1:2)
NR-C6(1:5)
PR-C6(1:2)
PR-C6(1:5)
AR-C6(1:2)
AR-C6(1:5)
NR
PR
AR
PEI

**Figure 5.** Luciferase transgene expression (RLU/mg) for lead lipopolymers, their corresponding parental polymers and PEI (25kDa) in **(A)** 22Rv1, **(B)** PC3-PSMA and **(C)** MB49 cells. Luciferase expression was determined for lipopolymer:pDNA weight ratios from 5:1 to 50:1. * = $p < 0.05$; ** = $p < 0.01$ using Student's *t*-test; p-values were obtained by comparing RLU/mg values of each lipopolymer and the parental polymers with PEI under corresponding conditions. Data represent mean ± one standard deviation of three independent experiments (n=3).

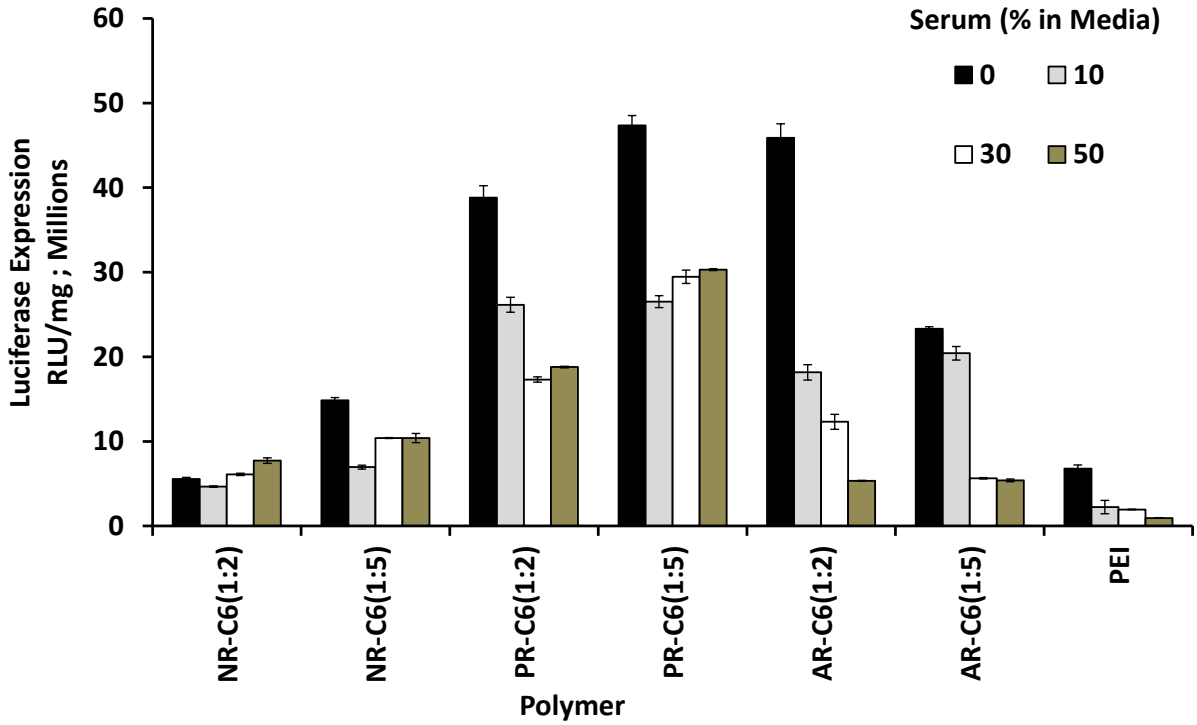


**Figure 6.** Luciferase transgene expression (RLU/mg) for lead LPNs and PEI (25 kDa, branched) in PC3 cells following delivery of pDNA in presence of increasing concentrations of serum in media. Efficacies of LPNs and PEI were investigated at optimal LPN:pDNA (w/w) ratios, based on the dose response study shown in Figure 4. Data represent mean ± one standard deviation of three independent experiments (n=3). Statistical analyses (Student's t-test) indicated that RLU/mg values for every LPN were statistically significant compared to PEI under corresponding conditions.

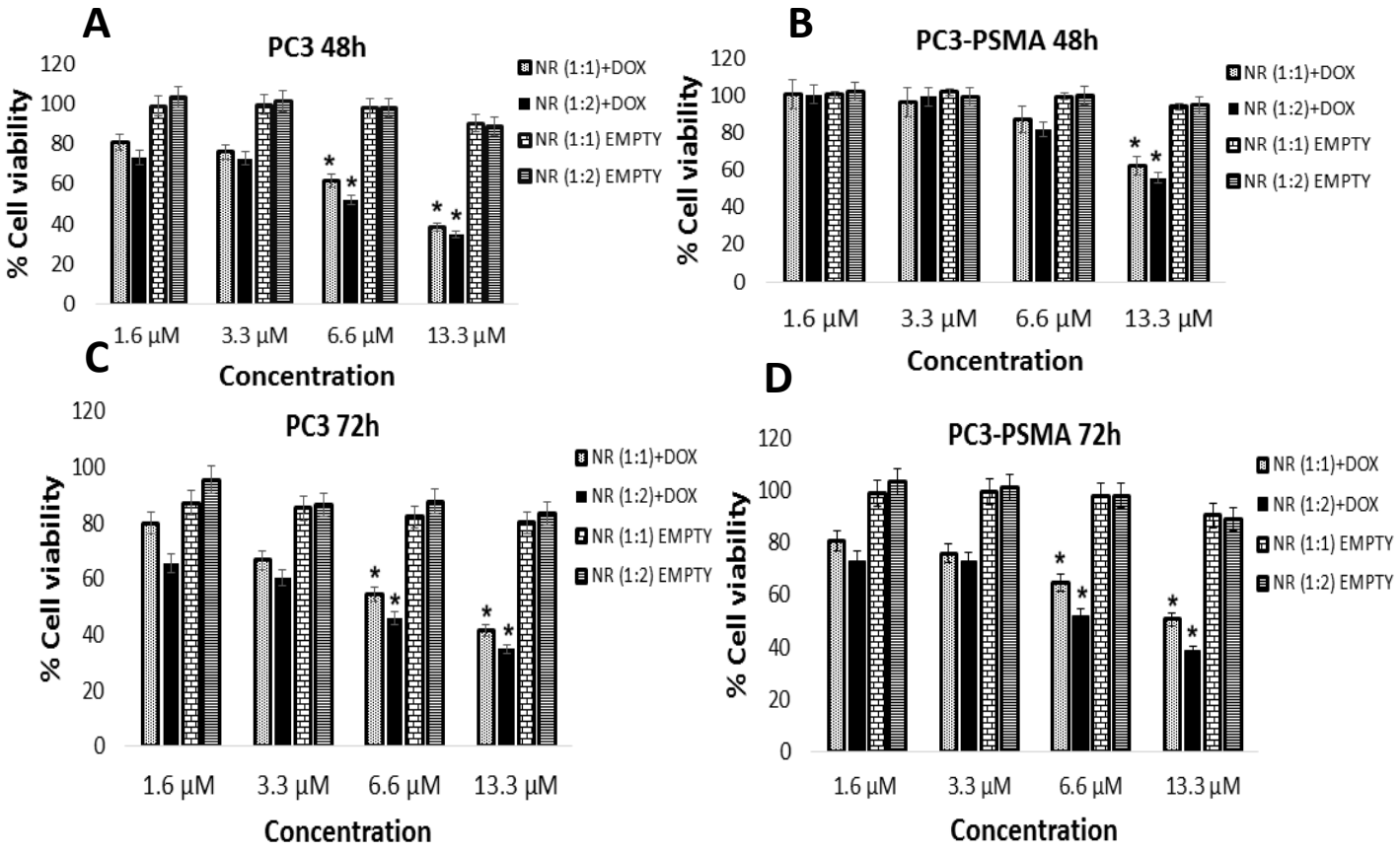


**Figure 7.** Cell viability of PC3 and PC3-PSMA cells following treatment with doxorubicin (DOX)-encapsulated LPNs at different concentrations. Cell viability was determined using the MTT assay, and in all cases, compared to empty (unencapsulated DOX nanoparticles) as the control. * = $p < 0.05$; using Student's *t*-test; p-values were obtained by comparing DOX-loaded nanoparticles with empty nanoparticles under corresponding conditions. Data represent mean ± one standard deviation of three independent experiments (n=3).

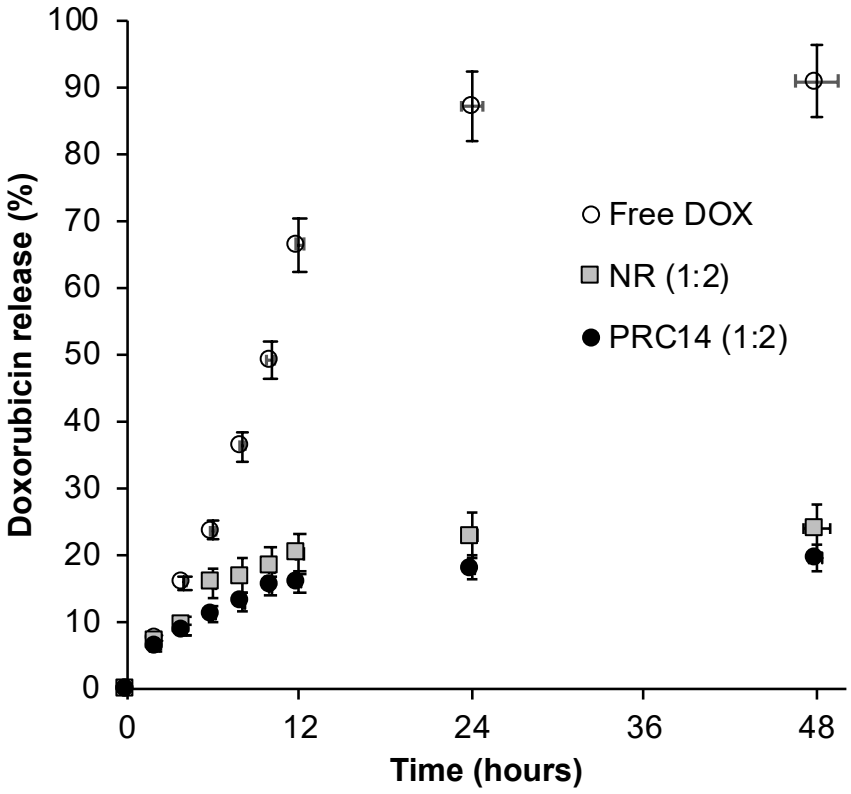


**Figure 8.** Kinetics of doxorubicin (DOX) release from NR (1:2), PR-C14 (1:2) LPNs in 10 mM HEPES (pH 7.4), compared to that of free doxorubicin from a 8-10 kDa molecular weight cutoff Float-A-Lyzer dialysis tubing into a 10 mM HEPES (pH 7.4) buffer. Methods are described in the experimental section.

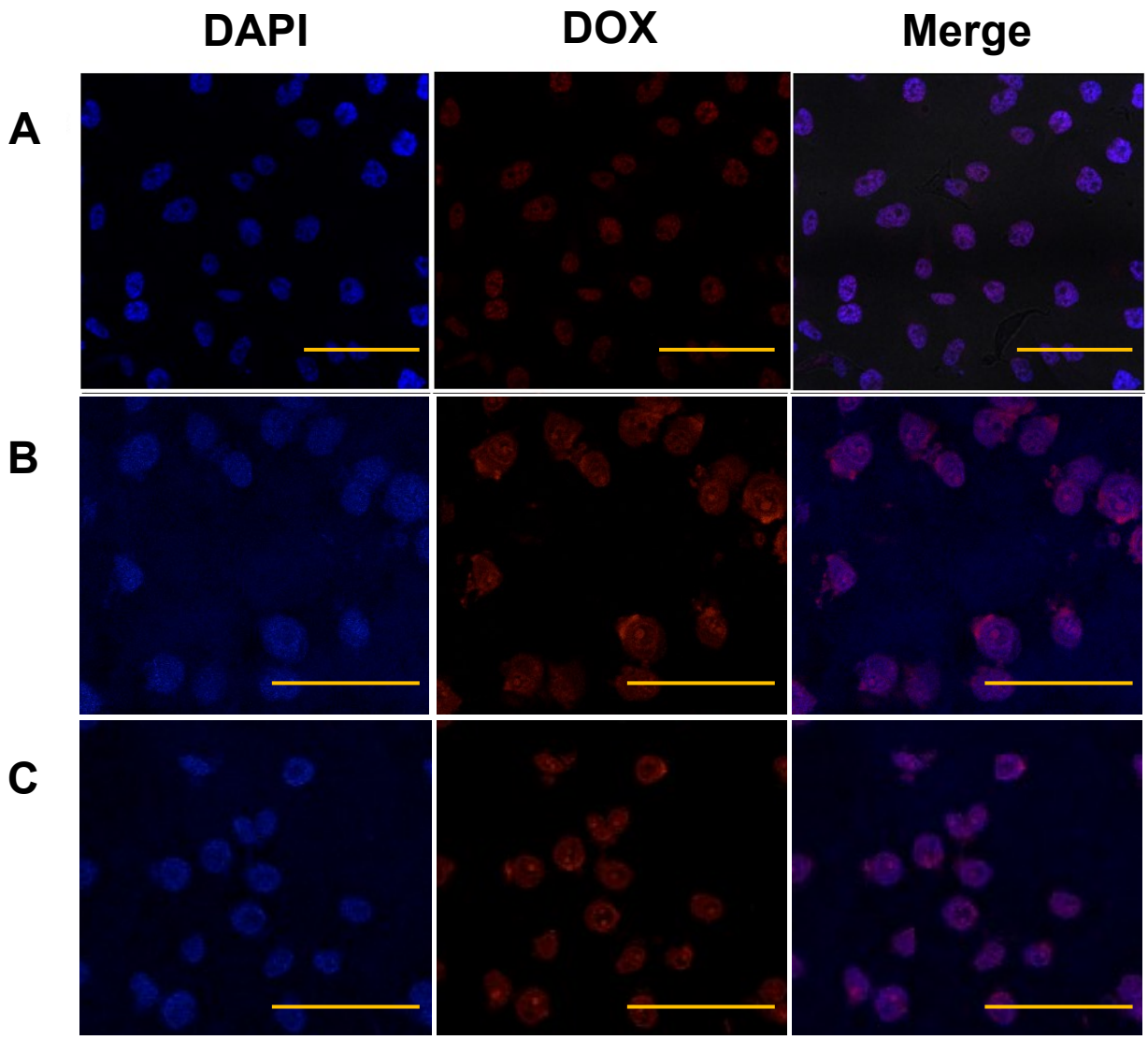


**Figure 9.** Confocal fluorescence microscopy images of PC3 cells following treatment with **(A)** free DOX, **(B)** DOX-loaded PR-C14 (1:2) LPN, and **(C)** DOX-loaded NR (1:2) parental polymer for 24h. Scale bar = 50 μm in all images.

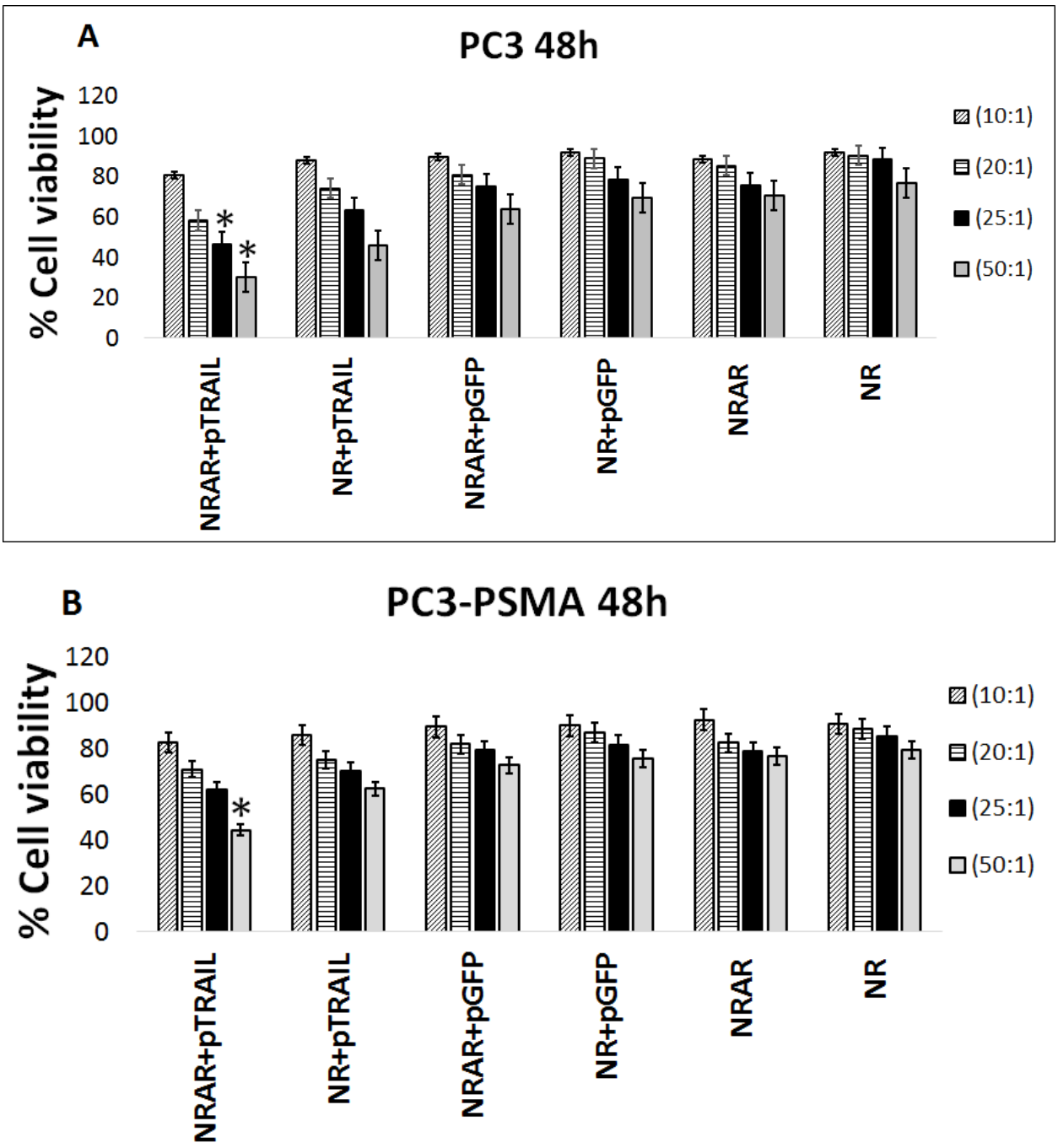


**Figure 10.** Simultaneous delivery of HDACi (AR-42) and plasmid DNA (pTRAIL) and evaluation of cell viability of **(A)** PC3 and **(B)** PC3-PSMA cells following treatment with NR polymeric nanoparticles at different polymer:pDNA weight ratios. Cell viability was determined using the MTT assay, and in all cases, compared to pGFP as the control. * = $p < 0.05$; using Student's *t*-test; p-values were obtained by comparing NRAR polymer:pTRAIL weight ratios with NRAR polymer:pGFP weight ratios under corresponding conditions. Data represent mean ± one standard deviation of three independent experiments (n=3).

## REFERENCES


1. Torchilin, V.P., *Multifunctional, stimuli-sensitive nanoparticulate systems for drug delivery.* ***Nat Rev Drug Discov***, **2014**. 13(11): 813-827.
2. Luk, B.T. and Zhang, L., *Current Advances in Polymer-Based Nanotheranostics for Cancer Treatment and Diagnosis.* ***ACS Applied Materials & Interfaces***, **2014**. 6(24): 21859-21873.
3. Babu, A., Templeton, A., Munshi, A., and Ramesh, R., *Nanodrug Delivery Systems: A Promising Technology for Detection, Diagnosis, and Treatment of Cancer.* ***AAPS PharmSciTech***, **2014**. 15(3): 709-721.
4. Bao, G., Mitragotri, S., and Tong, S., *Multifunctional Nanoparticles for Drug Delivery and Molecular Imaging.* ***Annual Review of Biomedical Engineering***, **2013**. 15(1): 253-282.
5. Li, J., Wang, Y., Zhu, Y., and Oupický, D., *Recent advances in delivery of drug–nucleic acid combinations for cancer treatment.* ***Journal of Controlled Release***, **2013**. 172(2): 589-600.
6. Vu, L., Ramos, J., Potta, T., and Rege, K., *Generation of a focused poly(amino ether) library: polymer-mediated transgene delivery and gold-nanorod based theranostic systems.* ***Theranostics***, **2012**. 2(12): 1160-73.
7. Dachs, G.U., Dougherty, G.J., Stratford, I.J., and Chaplin, D.J., *Targeting gene therapy to cancer: A review.* ***Oncology Research***, **1997**. 9(6-7): 313-325.
8. Izquierdo, M., *Short interfering RNAs as a tool for cancer gene therapy.* ***Cancer Gene Therapy***, **2005**. 12(3): 217-227.
9. Mercola, D. and Cohen, J.S., *ANTISENSE APPROACHES TO CANCER GENE-THERAPY.* ***Cancer Gene Therapy***, **1995**. 2(1): 47-59.
10. Zuckerman, J.E., Gritli, I., Tolcher, A., Heidel, J.D., Lim, D., Morgan, R., Chmielowski, B., Ribas, A., Davis, M.E., and Yen, Y., *Correlating animal and human phase Ia/Ib clinical data with CALAA-01, a targeted, polymer-based nanoparticle containing siRNA.* ***Proceedings of the National Academy of Sciences***, **2014**. 111(31): 11449-11454.
11. Roth, C.M. and Sundaram, S., *Engineering Synthetic Vectors for Improved DNA Delivery: Insights from Intracellular Pathways.* ***Annual Review of Biomedical Engineering***, **2004**. 6(1): 397-426.
12. Wang, Y., Gao, S.J., Ye, W.H., Yoon, H.S., and Yang, Y.Y., *Co-delivery of drugs and DNA from cationic core-shell nanoparticles self-assembled from a biodegradable copolymer.* ***Nature Materials***, **2006**. 5(10): 791-796.
13. Zhang, J.X., Sun, H.L., and Ma, P.X., *Host-Guest Interaction Mediated Polymeric Assemblies: Multifunctional Nanoparticles for Drug and Gene Delivery.* ***Acs Nano***, **2010**. 4(2): 1049-1059.
14. Qiu, L.Y. and Bae, Y.H., *Self-assembled polyethylenimine-graft-poly(epsilon-caprolactone) micelles as potential dual carriers of genes and anticancer drugs.* ***Biomaterials***, **2007**. 28(28): 4132-4142.
15. Kataoka, K., Harada, A., and Nagasaki, Y., *Block copolymer micelles for drug delivery: design, characterization and biological significance.* ***Advanced Drug Delivery Reviews***, **2001**. 47(1): 113-131.
16. Miryala, B., Godeshala, S., Grandhi, T.S., Christensen, M.D., Tian, Y., and Rege, K., *Aminoglycoside-derived amphiphilic nanoparticles for molecular delivery.* ***Colloids Surf B Biointerfaces***, **2016**. 146: 924-37.

17. Meka, R.R., Godeshala, S., Marepally, S., Thorat, K., Reddy Rachamalla, H.K., Dhayani, A., Hiwale, A., Banerjee, R., Chaudhuri, A., and Vemula, P.K., *Asymmetric cationic lipid based non-viral vectors for an efficient nucleic acid delivery.* ***RSC Advances***, **2016**. 6(81): 77841-77848.
18. Andey, T., Sudhakar, G., Marepally, S., Patel, A., Banerjee, R., and Singh, M., *Lipid nanocarriers of a lipid-conjugated estrogenic derivative inhibit tumor growth and enhance cisplatin activity against triple-negative breast cancer: pharmacokinetic and efficacy evaluation.* ***Mol Pharm***, **2015**. 12(4): 1105-20.
19. Li, F., Danquah, M., and Mahato, R.I., *Synthesis and characterization of amphiphilic lipopolymers for micellar drug delivery.* ***Biomacromolecules***, **2010**. 11(10): 2610-20.
20. Mangraviti, A., Tzeng, S.Y., Kozielski, K.L., Wang, Y., Jin, Y., Gullotti, D., Pedone, M., Buaron, N., Liu, A., Wilson, D.R., Hansen, S.K., Rodriguez, F.J., Gao, G.-D., DiMeco, F., Brem, H., Olivi, A., Tyler, B., and Green, J.J., *Polymeric Nanoparticles for Nonviral Gene Therapy Extend Brain Tumor Survival in Vivo.* ***ACS Nano***, **2015**. 9(2): 1236-1249.
21. Kim, C., Lee, S.C., Kang, S.W., Kwon, I.C., Kim, Y.-H., and Jeong, S.Y., *Synthesis and the Micellar Characteristics of Poly(ethylene oxide)−Deoxycholic Acid Conjugates1.* ***Langmuir***, **2000**. 16(11): 4792-4797.
22. Dheer, D., Arora, D., Jaglan, S., Rawal, R.K., and Shankar, R., *Polysaccharides based nanomaterials for targeted anti-cancer drug delivery.* ***Journal of Drug Targeting***, **2017**. 25(1): 1-16.
23. Swierczewska, M., Han, H.S., Kim, K., Park, J.H., and Lee, S., *Polysaccharide-based Nanoparticles for Theranostic Nanomedicine.* ***Advanced drug delivery reviews***, **2016**. 99(Pt A): 70-84.
24. Choi, K.Y., Chung, H., Min, K.H., Yoon, H.Y., Kim, K., Park, J.H., Kwon, I.C., and Jeong, S.Y., *Self-assembled hyaluronic acid nanoparticles for active tumor targeting.* ***Biomaterials***, **2010**. 31(1): 106-114.
25. Chen, C.-Y., Kim, T.H., Wu, W.-C., Huang, C.-M., Wei, H., Mount, C.W., Tian, Y., Jang, S.-H., Pun, S.H., and Jen, A.K.Y., *pH-Dependent, Thermosensitive Polymeric Nanocarriers for Drug Delivery to Solid Tumors.* ***Biomaterials***, **2013**. 34(18): 4501-4509.
26. Yoo, H.S. and Park, T.G., *Folate receptor targeted biodegradable polymeric doxorubicin micelles.* ***J Control Release***, **2004**. 96(2): 273-83.
27. Kim, S.H., Jeong, J.H., Kim, T.I., Kim, S.W., and Bull, D.A., *VEGF siRNA delivery system using arginine-grafted bioreducible poly(disulfide amine).* ***Mol Pharm***, **2009**. 6(3): 718-26.
28. Taori, V.P., Liu, Y.M., and Reineke, T.M., *DNA delivery in vitro via surface release from multilayer assemblies with poly(glycoamidoamine)s.* ***Acta Biomaterialia***, **2009**. 5(3): 925-933.
29. Davies, J. and Davis, B.D., *Misreading of ribonucleic acid code words induced by aminoglycoside antibiotics. The effect of drug concentration.* ***J Biol Chem***, **1968**. 243(12): 3312-6.
30. Moazed, D. and Noller, H.F., *Interaction of antibiotics with functional sites in 16S ribosomal RNA.* ***Nature***, **1987**. 327(6121): 389-94.
31. Ecker, D.J. and Griffey, R.H., *RNA as a small-molecule drug target: doubling the value of genomics.* ***Drug Discovery Today***, **1999**. 4(9): 420-429.
32. Zaman, G.J.R., Michiels, P.J.A., and van Boeckel, C.A.A., *Targeting RNA: new opportunities to address drugless targets.* ***Drug Discovery Today***, **2003**. 8(7): 297-306.

33. Luedtke, N.W., Baker, T.J., Goodman, M., and Tor, Y., *Guanidinoglycosides: A Novel Family of RNA Ligands.* ***Journal of the American Chemical Society***, **2000**. 122(48): 12035-12036.
34. Rege, K., Hu, S., Moore, J.A., Dordick, J.S., and Cramer, S.M., *Chemoenzymatic synthesis and high-throughput screening of an aminoglycoside-polyamine library: identification of high-affinity displacers and DNA-binding ligands.* ***J Am Chem Soc***, **2004**. 126(39): 12306-15.
35. Rege, K., Ladiwala, A., Hu, S., Breneman, C.M., Dordick, J.S., and Cramer, S.M., *Investigation of DNA-binding properties of an aminoglycoside-polyamine library using quantitative structure-activity relationship (QSAR) models.* ***J Chem Inf Model***, **2005**. 45(6): 1854-63.
36. Potta, T., Zhen, Z., Grandhi, T.S., Christensen, M.D., Ramos, J., Breneman, C.M., and Rege, K., *Discovery of antibiotics-derived polymers for gene delivery using combinatorial synthesis and cheminformatics modeling.* ***Biomaterials***, **2014**. 35(6): 1977-88.
37. Miryala, B., Feng, Y., Omer, A., Potta, T., and Rege, K., *Quaternization enhances the transgene expression efficacy of aminoglycoside-derived polymers.* ***International Journal of Pharmaceutics***, **2015**. 489(1–2): 18-29.
38. Miryala, B., Zhen, Z., Potta, T., Breneman, C.M., and Rege, K., *Parallel Synthesis and Quantitative Structure–Activity Relationship (QSAR) Modeling of Aminoglycoside-Derived Lipopolymers for Transgene Expression.* ***ACS Biomaterials Science & Engineering***, **2015**. 1(8): 656-668.
39. Gosnell, H., Kasman, L.M., Potta, T., Vu, L., Garrett-Mayer, E., Rege, K., and Voelkel-Johnson, C., *Polymer-enhanced delivery increases adenoviral gene expression in an orthotopic model of bladder cancer.* ***J Control Release***, **2014**. 176: 35-43.
40. Godeshala, S., Nitiyanandan, R., Thompson, B., Goklany, S., Nielsen, D., and Rege, K., *Folate receptor-targeted aminoglycoside-derived polymers for transgene expression in cancer cells*. 2016. 1(2), 220-231.
41. Pavan Grandhi, T.S., Potta, T., Nitiyanandan, R., Deshpande, I., and Rege, K., *Chemomechanically engineered 3D organotypic platforms of bladder cancer dormancy and reactivation.* ***Biomaterials***, **2017**. 142: 171-185.
42. Dobos, A., Grandhi, T.S.P., Godeshala, S., Meldrum, D.R., and Rege, K., *Parallel fabrication of macroporous scaffolds.* ***Biotechnology and Bioengineering***, **2018**. 0(0).
43. Kasman, L., Lu, P., and Voelkel-Johnson, C., *The histone deacetylase inhibitors depsipeptide and MS-275, enhance TRAIL gene therapy of LNCaP prostate cancer cells without adverse effects in normal prostate epithelial cells.* ***Cancer Gene Ther***, **2007**. 14(3): 327-34.
44. Hellwig, C.T. and Rehm, M., *TRAIL Signaling and Synergy Mechanisms Used in TRAIL-Based Combination Therapies.* ***Molecular Cancer Therapeutics***, **2012**. 11(1): 3.
45. Godeshala, S., Nitiyanandan, R., Thompson, B., Goklany, S., Nielsen, D.R., and Rege, K., *Folate receptor-targeted aminoglycoside-derived polymers for transgene expression in cancer cells.* ***Bioengineering & Translational Medicine***, **2016**. 1(2): 220-231.
46. Goklany, S., Lu, P., Godeshala, S., Hall, A., Garrett-Mayer, E., Voelkel-Johnson, C., and Rege, K., *Delivery of TRAIL-expressing plasmid DNA to cancer cells in vitro and in vivo using aminoglycoside-derived polymers.* ***J Mater Chem B***, **2019**. 7(44): 7014-7025.

47. Elshafae, S.M., Kohart, N.A., Altstadt, L.A., Dirksen, W.P., and Rosol, T.J., *The Effect of a Histone Deacetylase Inhibitor (AR-42) on Canine Prostate Cancer Growth and Metastasis.* ***The Prostate***, **2017**. 77(7): 776-793.
48. Elmer, J.J., Christensen, M.D., Barua, S., Lehrman, J., Haynes, K.A., and Rege, K., *The histone deacetylase inhibitor Entinostat enhances polymer-mediated transgene expression in cancer cell lines.* ***Biotechnol Bioeng***, **2016**. 113(6): 1345-56.
49. Barua, S. and Rege, K., *The influence of mediators of intracellular trafficking on transgene expression efficacy of polymer-plasmid DNA complexes.* ***Biomaterials***, **2010**. 31(22): 5894-902.
50. Rege, K., Hu, S., Moore, J.A., Dordick, J.S., and Cramer, S.M., *Chemoenzymatic Synthesis and High-Throughput Screening of an Aminoglycoside−Polyamine Library: Identification of High-Affinity Displacers and DNA-Binding Ligands.* ***Journal of the American Chemical Society***, **2004**. 126(39): 12306-12315.
51. Allen, C., Maysinger, D., and Eisenberg, A., *Nano-engineering block copolymer aggregates for drug delivery.* ***Colloids and Surfaces B: Biointerfaces***, **1999**. 16(1): 3-27.
52. Anderson, D.G., Akinc, A., Hossain, N., and Langer, R., *Structure/property studies of polymeric gene delivery using a library of poly(beta-amino esters).* ***Mol Ther***, **2005**. 11(3): 426-34.
53. Wang, M., Wu, B., Tucker, J.D., Lu, P., and Lu, Q., *Poly(ester amine) constructed from polyethylenimine and pluronic for gene delivery in vitro and in vivo.* ***Drug Delivery***, **2016**. 23(9): 3224-3233.
54. Yu, J., Xie, X., Wu, J., Liu, Y., Liu, P., Xu, X., Yu, H., Lu, L., and Che, X., *Folic acid conjugated glycol chitosan micelles for targeted delivery of doxorubicin: preparation and preliminary evaluation in vitro.* ***J Biomater Sci Polym Ed***, **2013**. 24(5): 606-20.
55. Lorenz, C., Hadwiger, P., John, M., Vornlocher, H.P., and Unverzagt, C., *Steroid and lipid conjugates of siRNAs to enhance cellular uptake and gene silencing in liver cells.* ***Bioorg Med Chem Lett***, **2004**. 14(19): 4975-7.
56. Wolfrum, C., Shi, S., Jayaprakash, K.N., Jayaraman, M., Wang, G., Pandey, R.K., Rajeev, K.G., Nakayama, T., Charrise, K., Ndungo, E.M., Zimmermann, T., Koteliansky, V., Manoharan, M., and Stoffel, M., *Mechanisms and optimization of in vivo delivery of lipophilic siRNAs.* ***Nat Biotechnol***, **2007**. 25(10): 1149-57.
57. Nishina, K., Unno, T., Uno, Y., Kubodera, T., Kanouchi, T., Mizusawa, H., and Yokota, T., *Efficient in vivo delivery of siRNA to the liver by conjugation of alpha-tocopherol.* ***Mol Ther***, **2008**. 16(4): 734-40.
58. Soutschek, J., Akinc, A., Bramlage, B., Charisse, K., Constien, R., Donoghue, M., Elbashir, S., Geick, A., Hadwiger, P., Harborth, J., John, M., Kesavan, V., Lavine, G., Pandey, R.K., Racie, T., Rajeev, K.G., Rohl, I., Toudjarska, I., Wang, G., Wuschko, S., Bumcrot, D., Koteliansky, V., Limmer, S., Manoharan, M., and Vornlocher, H.P., *Therapeutic silencing of an endogenous gene by systemic administration of modified siRNAs.* ***Nature***, **2004**. 432(7014): 173-8.
59. Neamnark, A., Suwantong, O., K. C, R.B., Hsu, C.Y.M., Supaphol, P., and Uludağ, H., *Aliphatic Lipid Substitution on 2 kDa Polyethylenimine Improves Plasmid Delivery and Transgene Expression.* ***Molecular Pharmaceutics***, **2009**. 6(6): 1798-1815.
60. Doody, A.M., Korley, J.N., Dang, K.P., Zawaneh, P.N., and Putnam, D., *Characterizing the structure/function parameter space of hydrocarbon-conjugated branched*

*polyethylenimine for DNA delivery in vitro.* ***Journal of Controlled Release***, **2006**. 116(2): 227-237.

61. Yi, W.-J., Zhang, Q.-F., Zhang, J., Liu, Q., Ren, L., Chen, Q.-M., Guo, L., and Yu, X.-Q., *Cyclen-based lipidic oligomers as potential gene delivery vehicles.* ***Acta Biomaterialia***, **2014**. 10(3): 1412-1422.
62. Matsui, K., Sando, S., Sera, T., Aoyama, Y., Sasaki, Y., Komatsu, T., Terashima, T., and Kikuchi, J.-i., *Cerasome as an Infusible, Cell-Friendly, and Serum-Compatible Transfection Agent in a Viral Size.* ***Journal of the American Chemical Society***, **2006**. 128(10): 3114-3115.
63. Zhang, C., Tang, N., Liu, X., Liang, W., Xu, W., and Torchilin, V.P., *siRNA-containing liposomes modified with polyarginine effectively silence the targeted gene.* ***J Control Release***, **2006**. 112(2): 229-39.
64. Ogris, M., Brunner, S., Schuller, S., Kircheis, R., and Wagner, E., *PEGylated DNA/transferrin-PEI complexes: reduced interaction with blood components, extended circulation in blood and potential for systemic gene delivery.* ***Gene Ther***, **1999**. 6(4): 595-605.
65. Thomas, M., Ge, Q., Lu, J.J., Chen, J., and Klibanov, A.M., *Cross-linked small polyethylenimines: while still nontoxic, deliver DNA efficiently to mammalian cells in vitro and in vivo.* ***Pharm Res***, **2005**. 22(3): 373-80.
66. Forrest, M.L., Meister, G.E., Koerber, J.T., and Pack, D.W., *Partial acetylation of polyethylenimine enhances in vitro gene delivery.* ***Pharm Res***, **2004**. 21(2): 365-71.
67. Dai, X., Yue, Z., Eccleston, M.E., Swartling, J., Slater, N.K., and Kaminski, C.F., *Fluorescence intensity and lifetime imaging of free and micellar-encapsulated doxorubicin in living cells.* ***Nanomedicine***, **2008**. 4(1): 49-56.
68. Lai, Y., Lei, Y., Xu, X., Li, Y., He, B., and Gu, Z., *Polymeric micelles with [small pi]-[small pi] conjugated cinnamic acid as lipophilic moieties for doxorubicin delivery.* ***Journal of Materials Chemistry B***, **2013**. 1(34): 4289-4296.